

Coordination Chemistry of Bithiazole Ligands: A  
Comparative Study of the 2,2' and 4,4' Isomers

A Thesis

Presented to the

Department of Chemistry

Of

Lakehead University

By

Jamila Marroush

In partial fulfillment of a requirement for the degree of

Master of Chemistry

## Abstract

The bithiazole ring system consists of two thiazole ( $C_3NS$ ) aromatic rings. There are many regioisomers but two of potential interest for coordination chemistry are the 2,2'-bis(1,3-thiazole) and the 4,4'-bis(1,3-thiazole), because in the syn orientation they have a bipyridyl-like core that could lead to chelating behaviour. Very few single-crystal structures are known to contain bithiazole ligands and those that are known, are mostly of the 4,4'-isomer. This thesis presents work on new ligands using the bithiazole core, reporting the synthesis and coordination chemistry of 2,2'-dichloro-4,4'-bithiazole, 5,5'-dibromo-2,2'-dimethyl-4,4'-bithiazole, and 5,5'-dibromo-2,2'-diamino-4,4' bithiazole. In solution, the bithiazole ligands are weaker ligands than bipyridyl ligands, but when used in large-scale, and high concentration reactions, a coordination complex can be isolated. UV-vis and combustion analysis evidence are reported to support the formation of the coordination complex. In the case of coordination compounds between silver(I) and a 5,5'-dicyano-2,2'-bithiazoles core, thermogravimetric analysis, differential scanning calorimetry, and X-ray powder diffraction are used to characterize the thermal stability of the known single-crystal structures.

## Acknowledgments

In the name of Allah, the Most Gracious and the Most Merciful, Alhamdulillah, all praises are given to Allah for the strengths and His blessing in completing this thesis. First, I must express my gratitude to my supervisor Dr. Craig MacKinnon.

Dr. Mackinnon helps me to all questions regarding my research and writing. This thesis would never have been completed without his support and encouragement.

Next, I would also like to extend appreciation my committee members Dr. Christine Gottardo and Dr. Michael Campbell of the Faculty of Science and Environmental Studies at Lakehead University. For all their help and valuable comments on this thesis.

Special appreciation goes to Debbie Puumala at the chemical store for fixing everything and answering all my questions. Also, Michael Sorokopud of the Instrumentation Laboratory for his assistance with NMR spectroscopy and X-Ray diffraction.

Finally, I also would like to acknowledge the Canadian Bureau for International Education for giving me the opportunity to complete my MSc degree and their financial support during my academic years at Lakehead University.

## **To my family**

I must express profound gratitude to my parents and my husband's mother they have always believed in me. Moreover, I cannot forget to thank my husband, Mohamed to help me to take care of my children Abdurrahim and Abdurrahman, and my friends for their patience and for providing me with support and continues encouragement throughout my years of study. This research would not have been completed without them.

# Table of Contents

<b>List of Abbreviations</b> .....	<b>vii</b>
<b>List of Figures</b> .....	<b>x</b>
<b>List of Schemes</b> .....	<b>xii</b>
<b>List of Tables</b> .....	<b>xiii</b>
<b>Chapter 1-Introduction</b> .....	<b>1</b>
1.1 Metals in molecular chemistry .....	1
1.2 The Hard-Soft Acid-Base (HSAB) Model .....	2
1.3 Survey of ligands .....	3
1.3.1 Chelate Effects.....	3
1.3.2 Back-bonding .....	4
1.3.3 Carbon Monoxide .....	4
1.3.4 Phosphine Ligands.....	5
1.3.5 1,2-bis(diphenylphosphino)ethane Ligand .....	5
1.3.6 Nitrogen-containing Heterocyclic rings .....	5
1.3.6.1 2,2'-Bipyridine Ligand .....	6
1.3.6.2 Phenanthroline ligand.....	7
1.3.6.3 Porphyrin ligand .....	7
1.4 The Bithiazole Ring System .....	8
1.4.1 Medical uses of bithiazole .....	9
1.4.2 Materials applications of bithiazole .....	11
1.4.3 Coordination chemistry of bithiazole.....	11
1.5 Coordination polymers and metal-organic frameworks .....	12
1.5.1 Extended structures using silver(I) with organic nitriles .....	12
1.6 General goals of this thesis.....	13
<b>Chapter 2-Ligand Synthesis</b> .....	<b>14</b>
2.1 Introduction to 2,2'-bithiazole and 4,4'-bithiazole .....	14
2.2 The Hantzsch Thiazole Synthesis .....	15
2.2.1 Proposed ligand comparison .....	16
2.3 Synthesis of Ligand Target .....	17
2.3.1 Synthesis of 1,4-dibromo-2,3-butanedione .....	17
2.3.2 Ring-closing Syntheses of 4,4'-Bithiazoles .....	17
2.3.3 Ring-closing Syntheses of 2,2'-Bithiazole.....	18

2.3.4 Synthesis of Dicyanobithiazoles .....	19
2.4 Conclusion .....	23
2.5 Experimental .....	23
2.5.1 Instrumentation .....	23
2.5.2 General Synthesis.....	24
2.5.3 Preparation of 2,2'-dichloro-4,4'-bithiazole (5) .....	24
2.5.4 Preparation of 2,2'-dicyano-4,4'-bithiazole.....	25
(a) Rosamund-von Braun route .....	25
(b) Sandmeyer route.....	25
2.5.5 Preparation of 5,5'-dibromo-2,2'-dimethyl-4,4'-bithiazole .....	26
2.5.6 Preparation of 5,5'-dibromo-2,2'-diamino-4,4'-bithiazole.....	26
<b>Chapter 3-Comparison of Bithiazole Regioisomers as Ligands .....</b>	<b>27</b>
3.1 Introduction to a systematic comparison of 4,4' vs 2,2' with metals .....	27
3.2 Attempted characterization of bithiazole coordination compounds in solution .....	29
3.2.1 Testing of ligand-metal solutions in acetonitrile and ethanol.....	30
3.3 Isolation of Methylbithiazole Complexes .....	32
3.3.1 Synthesis of Methylbithiazole Complexes .....	33
3.3.2 Result and discussion .....	33
3.4 Experimental .....	35
3.4.1 General considerations .....	35
3.4.2 UV-visible absorption experiments .....	35
3.4.3 Isolation of bithiazole-metal complexes .....	36
3.4.3.1 Me-4-Tz with NiSO <sub>4</sub> •6H <sub>2</sub> O.....	36
3.4.3.2 Me-4Tz with CoSO <sub>4</sub> •7H <sub>2</sub> O.....	37
3.4.3.3 Me-4Tz with FeSO <sub>4</sub> •7H <sub>2</sub> O .....	37
3.4.3.4 Me-4-Tz with Fe <sub>2</sub> (SO <sub>4</sub> ) <sub>3</sub> .....	37
3.4.3.5 Me-4-Tz with YCl <sub>3</sub> .....	38
3.4.3.6 Me-4-Tz with MnSO <sub>4</sub> •H <sub>2</sub> O .....	38
3.4.3.7 Me-4-Tz with CuSO <sub>4</sub> •5H <sub>2</sub> O.....	39
<b>Chapter 4-Ag(I) coordination compounds with bithiazole dinitriles .....</b>	<b>40</b>
4.1 Ag(I) coordination.....	40
4.1.1 Alkyl dinitriles .....	40
4.1.2 Phenyl nitriles.....	40
4.1.3 Coordination-active bridges.....	41

4.2 General synthesis of Ag(I) dinitrile coordination complexes .....	42
4.3 Results and Discussion .....	42
4.3.1 DSC analysis .....	51
4.3.2 XRD .....	52
4.4 Conclusion .....	55
4.5 Experimental .....	55
4.5.1 Instrumental techniques used.....	55
4.5.2 Synthesis – general procedures and materials .....	56
4.5.3 Synthesis of coordination compounds .....	56
<b>Chapter 5-General Conclusions and Future Direction .....</b>	<b>58</b>
5.1 Conclusion .....	58
5.2 Future directions .....	60
5.2.1 Direct continued work.....	60
5.2.2. Potential future projects.....	60
<b>Chapter 6-References .....</b>	<b>62</b>
<b>Appendix-Appendix 1: Literature syntheses as performed for this thesis .....</b>	<b>67</b>
A1.1 Preparation of 2,2'-dimethyl-4,4'-bithiazole <sup>14,35</sup> .....	67
A1.2 Preparation of 2,2'-diamino-4,4'-bithiazole <sup>36</sup> .....	67
A1.3 Preparation of 4,4'-dimethyl-2,2'-bithiazole <sup>37</sup> .....	68

## List of Abbreviations

A	absorbance
Bipy	bipyridine
BLM	bleomycin
Br <sub>2</sub>	bromine
°C	degrees Celsius
cm <sup>-1</sup>	wavenumber
DSC	differential scanning calorimetry
d	doublet (NMR descriptor)
DMF	<i>N, N</i> -dimethylformamide
d-DMSO	deuterated dimethylsulphoxide
dppe	1,2-bis(diphenylphosphino)ethane
EAN	Effective atomic number
Et <sub>2</sub> O	diethyl ether
EtOH	ethanol
g	gram
GAA	glacial acetic acid
IR	infrared spectroscopy



J	NMR coupling constant
LUIL	Lakehead University Instrumentation Laboratory
M	molarity
Me	methyl
Me-bipy	methylbipyridine
MeOH	methanol
mL	millilitre
mmol	millimole
MOFs	Metal-organic frameworks
mol	moles
N <sub>2</sub>	nitrogen
NBS	N-bromosuccinimide
nm	nanometer (wavelength)
NMR	nuclear magnetic resonance
t-BuONO	tert-Butyl nitrite
phen	phenanthroline
redox	Oxidation reduction
s	singlet (NMR descriptor)

S <sub>N</sub> 2	bimolecular nucleophilic substitution
t	triplet (NMR descriptor)
TGA	thermogravimetric analysis
THF	tetrahydrofuran
TF	thin film
2-Tz	2,2'-bithiazole
4-Tz	4,4'-bithiazole
UV-Vis	Ultraviolet–visible spectroscopy
XRD	X-ray powder diffraction
δ	NMR chemical shift

## List of Figures

<i>Figure 1.1:</i> Metal cation in an octahedral and a tetrahedral field.....	2
<i>Figure 1.2:</i> Electron bonding lone pair and back bonding.....	4
<i>Figure 1.3:</i> dppe ligand as a chelate to a single metal (left) and bridging two metals (right).....	5
<i>Figure 1.4:</i> Bipy Ligand.....	6
<i>Figure 1.5:</i> Phen Ligand.....	7
<i>Figure 1.6:</i> Heme Ligand.....	8
<i>Figure 1.7:</i> The 2-TZ and 4-TZ isomers of bithiazole .....	8
<i>Figure 1.8:</i> Acid base coordination chemistry in bithiazole metal polymers.....	9
<i>Figure 1.9:</i> Bithiazole domain of bleomycin.....	10
<i>Figure 4.1:</i> Ligands used in this study.....	42
<i>Figure 4.2:</i> Single crystal structure of $T_2CN_2+AgOTF$ ( $C_6H_6$ solvent) unit cell.....	44
<i>Figure 4.3:</i> TGA and DSC for Compound <b>12</b> .....	46
<i>Figure 4.4:</i> TGA and DSC for Compound <b>13</b> .....	47
<i>Figure 4.5:</i> TGA and DSC for Compound <b>14</b> .....	47
<i>Figure 4.6:</i> TGA and DSC for Compound <b>15</b> .....	48
<i>Figure 4.7:</i> TGA and DSC for Compound <b>16</b> .....	48

<i>Figure 4.8: TGA and DSC for Compound 17</i> .....	49
<i>Figure 4.9: TGA and DSC for Compound 18</i> .....	49
<i>Figure 4.10: TGA and DSC for Compound 19</i> .....	50
<i>Figure 4.11: TGA and DSC for Compound 20</i> .....	50
<i>Figure 4.12: TGA and DSC for Compound 21</i> .....	51
<i>Figure 4.13: Compound 12</i> .....	54
<i>Figure 4.14: Compound 18</i> .....	54

## List of Schemes

<i>Scheme 2.1:</i> Formation of a Thiazole using the Hantzsch Thiazole Synthesis.....	15
<i>Scheme 2.2:</i> Mechanism of the Hantzsch Thiazole Synthesis.....	16
<i>Scheme 2.3:</i> The synthesis of 1,4-dibromo-2,3-butanedione.....	17
<i>Scheme 2.4:</i> The synthesis of 2,2'-dimethyl-4,4'-bithiazole.....	18
<i>Scheme 2.5:</i> The synthesis of 2,2'-diamino-4,4'-bithiazole.....	18
<i>Scheme 2.6:</i> The synthesis of 4,4'-dimethyl-2,2'-bithiazole.....	18
<i>Scheme 2.7:</i> Bromination of 2,2'-dimethyl-4,4'-bithiazole.....	19
<i>Scheme 2.8:</i> Bromination of 2,2'-diamino-4,4'-bithiazole.....	20
<i>Scheme 2.9:</i> Deamination of 2,2'-dichloro-4,4'-bithiazole.....	21
<i>Scheme 2.10:</i> Cyanation of 2,2'-dichloro-4,4'-bithiazole.....	22
<i>Scheme 2.11:</i> Cyanation of 2,2'-diamino-4,4'-bithiazole.....	22
<i>Scheme 3.1:</i> Synthesis of bithiazoles.....	27
<i>Scheme 3.2:</i> The bithiazole binds as an N, N-chelate with metal.....	28

## List of Tables

<i>Table 3.1:</i> The UV-Vis peaks of the ligand-metal solutions in acetonitrile and ethanol using Me-bipy as ligand in a 1:1 ratio (compared to 280.0 nm, 269.0 nm) .....	30
<i>Table 3.2:</i> The UV-Vis peaks of the ligand-metal solutions in acetonitrile and ethanol using Me-4-Tz as ligand in a 1:1 ratio (compared to 262.0 nm, 262.0 nm) .....	31
<i>Table 3.3:</i> Combustion analysis results of 2,2'-dimethyl-4,4'-bithiazole ligand with different salt.....	34
<i>Table 4.1:</i> Structure of MOFs synthesized for this study (ratios are those observed in the single-crystal X-ray structure) .....	43
<i>Table 4.2:</i> TGA results.....	45
<i>Table 4.3:</i> XRD result for all complexes after heating.....	52

# Chapter 1

## Introduction

### 1.1 Metals in molecular chemistry

Modern inorganic chemistry, as distinct from geology or metallurgy, began with the Werner “coordination complexes”.<sup>1</sup> Many of the properties of these complexes can be modelled using Ligand Field Theory, especially those properties that depend on the metal *d*-orbitals such as colour and magnetism. Ligand field theory is an easily-understood model. The basic principle of this theory is metal-ligand interaction based on the electrostatic properties of metal cations and the surrounding electrostatic field generated by the ligand lone pairs of electrons. This kind of bonding is distinct from the covalent bonding found in organometallic complexes governed by the EAN (18-electron) rules. The relation of electrostatic attraction of ligand and metal cations is given as

$$E_{elec} = \frac{1}{4\pi\epsilon_0} \sum_{Ligands} \frac{q_M q_L}{\gamma_{ML}}$$

In terms of molecular orbital theory, the ligands donate an electron pair to a vacant orbital of appropriate symmetry on the metal. This creates a pair of new, highly polarized molecular orbitals. In such a system, the bonding orbitals are a combination of p orbital-based lone pairs on the ligands interaction with metal *d* orbitals, which are strongly polarized toward the ligand. The remaining orbitals (non- and antibonding combinations) can be described as primarily metal-based. Their energies are not equivalent, but rather they split into a characteristic pattern dependent on the molecular geometry; two examples are shown in **figure1.1**.

The ions or molecules linked to these metals are known as ligands and the number of bonds that each metal forms are known as the coordination number.<sup>2</sup>

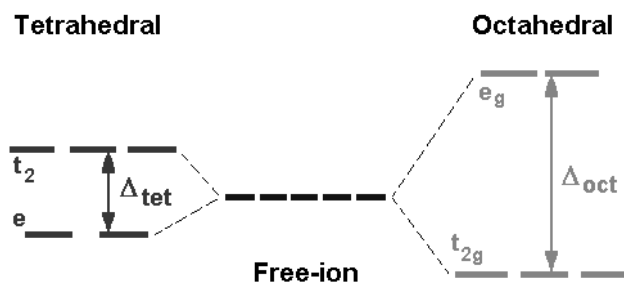


Figure 1.1: Metal cation in an octahedral and a tetrahedral field

## 1.2 The Hard-Soft Acid-Base (HSAB) Model

Not all metal cations form strong bonds with all possible ligands as both are selective, that is, some metals have a greater attraction to form coordination complexes with certain ligand types than others. It is therefore important to classify the ligands; one such system classifies the metals into hard and soft acids, and ligands into hard and soft bases. Charged metal ions with smaller or heavily charged atoms are called hard acids that have high charge densities. Hard acids prefer to bind to hard bases; this results in compounds with predominantly ionic bonding, i.e. the acid-base interaction does not form an explicit metal-ligand coordination bond.

Generally, hard bases are smaller anions, e.g.  $O^{2-}$  or  $F^-$ . Conversely, larger or more polarizable metallic cations with low charge density are called soft acids. In this case, polarizable means that they have large distortable clouds of electrons. Similarly, soft bases will be large polarizable anions with low charge densities. Unlike the hard acid-



base bonding, the bonds developed in this type of interaction have a significant amount of covalent character. There is a higher tendency that soft bases bind to soft acids.<sup>3</sup>

The HSAB principle can be used to rationalize geological features such as metal mineral preferences. For example, mercury will form sulfide minerals, while titanium is most commonly found as oxides like rutile. It can also be used to predict bonding in ambidentate ligands like cyanate  $\text{OCN}^-$ , where the oxygen lone pairs are harder and therefore more likely to bond to a hard acid, while soft acids will form bonds with the nitrogen end.

## **1.3 Survey of ligands**

### **1.3.1 Chelate Effects**

Chelation refers to the formation of coordinate bonds between a polydentate ligand around central metal atom. The ligands are generally organic compounds which coordinate with a metal ultimately forming a coordination complex. The chelate effect explains the attraction of chelating ligands to the metal. There is a thermodynamic preference for forming a chelate over the same number of bonds using monodentate ligands, e.g. one 1,2-diaminoethane (en) ligand is more favorable than bonding to two ammonia ligands.<sup>4</sup>

The thermodynamic origin of the chelate effect lies in the entropy of the reaction. For ligands of similar donor atoms (and therefore similar enthalpies of binding), the chelating ligand has a smaller entropy penalty than an equivalent set of monodentate ligands (less negative entropy of reaction), and therefore a more favorable Gibb's Free Energy of reaction. There is also a kinetic factor, since all the ligand donors in a chelate are

automatically in close approximation, once one donor binds to the metal the others will immediately attach.

### 1.3.2 Back-bonding

Back bonding, also called  $\pi$ -acidity, occurs when electron density from the metal is back-donated to an empty orbital on the ligand. An antibonding  $\pi$ -orbital on the organic group becomes filled. This concept in coordination chemistry is termed as back bonding as electron density is transferred back to the organic group, strengthening the metal-ligand bond.

### 1.3.3 Carbon Monoxide

Carbonyl complexes are those ligands in which a metal coordinates and interacts with a carbon monoxide group. CO is the classic  $\pi$ -acid system, namely an electron-bonding lone pair donation from the CO and back bonding from the metal to the CO  $\pi^*$  level. The figure below represents the concept of the above two components of CO bonding.

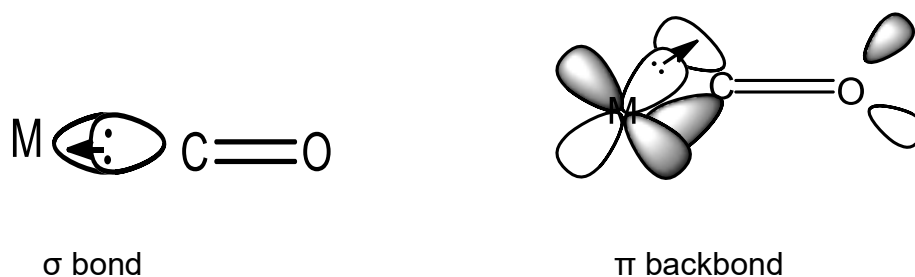


Figure 1.2: Electron bonding lone pair and back bonding

### 1.3.4 Phosphine Ligands

Phosphorus is considered one of the best elements with respect to electron donation in coordination chemistry. As a result, phosphines,  $\text{PR}_3$ , are a major class of ligands. The lone pair on the phosphorus atom forms strong bonds with soft metals and similar atoms having low oxidation states. Phosphorus acts as an electron donor to the coordinating metal cation. A vacant d-orbital on the atom can also serve as an electron acceptor, allowing phosphines to act as a  $\pi$ -acid ligand. Although these ligands are very common and useful, they are beyond the scope of this thesis.

### 1.3.5 1,2-bis(diphenylphosphino)ethane Ligand

The 1,2-bis(diphenylphosphino)ethane ligand (dppe), is an organophosphorus ligand. In coordination chemistry there is also the possibility of bridging two metal centers. The figure below represents the dppe ligand in two different bonding modes: as a chelate binding twice to the same metal cation, and as a bridge with each phosphorus donor binding to a different metal center.<sup>5</sup>



Figure 1.3: dppe ligand as a chelate to a single metal (left) and bridging two metals (right)

### 1.3.6 Nitrogen-containing Heterocyclic rings

Heterocyclic organic ring systems consist of carbon and at least one other non-carbon atom in the ring structure. The cyclic region of the compound demonstrates the presence

of one or more rings.<sup>6</sup> The most common structures noted are either five or six-membered ring structures and the most common examples containing only carbon and nitrogen are pyridine and pyrrole. There are many more examples of nitrogen-containing heterocyclic rings, both aromatic and non-aromatic, that may be synthesized or exist in nature.<sup>7</sup>

### 1.3.6.1 2,2'-Bipyridine Ligand

The 2,2'-bipyridyl (bipy) unit is one of the most used and researched ligands due to its ability to form a coordination complex with almost every metal. As can be seen in **Figure 1.4**, it is composed of two nitrogen-containing aromatic six-membered heterocyclic rings. It has been used over 100 years as a bidentate heterocyclic chelating ligand in organometallic and coordination chemistry. Bipyridine exists in six isomers but 2,2'-bipyridine is the one most used for coordination chemistry due to its functionality (being the only isomer that allows a chelate forming a 5-membered metalloheterocycle), and redox stability. Functionalized 2,2'-bipyridines have a wide range of applications in many areas of chemistry.<sup>8</sup>

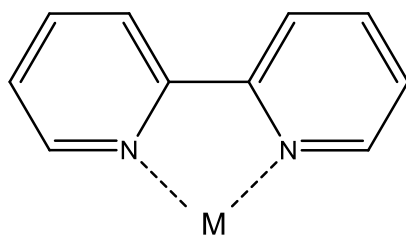


Figure 1.4: 2,2'-Bipyridine Ligand

### 1.3.6.2 Phenanthroline ligand

Phenanthroline (phen) is structurally similar to bipy but often forms stronger bonds with quicker reaction times. 1,10-phenanthroline is the most common due to its structure and the placement of the nitrogen atoms.<sup>9</sup>

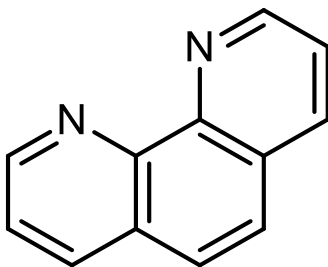


Figure 1.5: Phen Ligand

### 1.3.6.3 Porphyrin ligand

Heme is an important kind of polydentate ligand which is found in numerous biological molecules including hemoglobin in the blood, cytochrome enzymes, nitric oxide synthase, and many others. Hemoglobin consists of tetradentate nitrogen-containing macrocycle heme which coordinates with an iron ion to bind with an oxygen molecule. The macrocyclic ring itself is called a porphyrin; such ligands are natural chelating agents which can coordinate with a metal using the lone pairs on its four nitrogen atoms. The figure below illustrates the heme ligand.

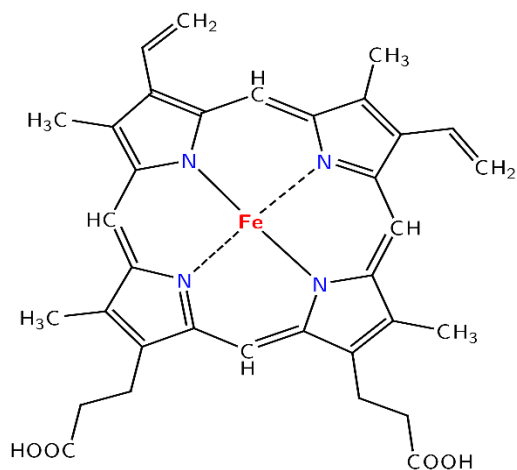


Figure 1.6: Appears to show an iron complex of the Heme Ligand

## 1.4 The Bithiazole Ring System

As seen from section 1.3, there are a wide variety of ligands with different donor atom sites. Ligands containing multiple types of donors are also possible. One such ligand system are the bithiazoles. This ring system has various isomers, two of which are shown in **Figure 1.7**. Although much less common than other heterocyclic ring systems, this moiety appears in several important biological systems, pharmaceuticals, and has potential as a ligand in coordination chemistry.

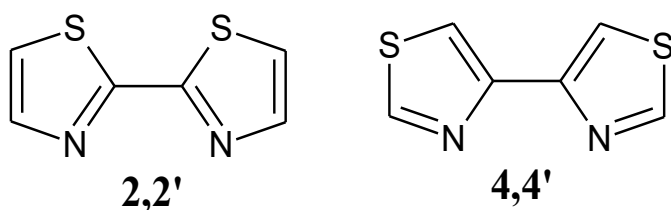


Figure 1.7: The 2-TZ and 4-TZ isomers of bithiazole

The figure above illustrates the heterocyclic rings of bithiazole with the possible sites to which a metal could coordinate. 2,2'-bithiazole is written as 2-Tz and 4,4'-bithiazole is called 4-Tz. It is anticipated that both of these isomers would bind to silver metal cations and will probably and preferably coordinate at nitrogen groups by analogy with bipy. However, using the HSAB model, the situation reveals itself to be more complex. Silver(I) is commonly considered soft, while sulfur in a ring like bithiazole would also be considered soft. Therefore, the HSAB model suggests that there is at least the possibility of binding to the sulfur in a heterocyclic ring containing a sulfur atom. There are published crystal structures containing a metal-thiophene interaction bound through the thiophene sulfur.<sup>20</sup>

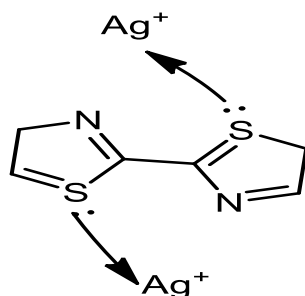


Figure 1.8: Acid base coordination chemistry in bithiazole metal polymers

#### 1.4.1 Medical uses of bithiazole

The thiazole ring system appears in a number of therapeutic agents, some of which are natural products. It is contained in drugs for Alzheimer's Disease,<sup>10</sup> anti-prion,<sup>11</sup> and anti-cancer treatments.<sup>12</sup> One particularly well-studied example is bleomycin (BLM). The bithiazole moiety, one domain of bleomycin, was shown to be responsible for binding of BLM to DNA, which plays an important role in the interaction of bleomycin with DNA.<sup>13-15</sup> Bleomycin is a glycopeptide antibiotic and is classified as an antitumor(anticancer)

antibiotic in the medical sciences. It produces single- and double-strand breaks in DNA.<sup>15</sup> Bleomycin is used for the treatment of sarcoma, squamous cell carcinomas, lymphomas, and testicular cancer. Bleomycin can also be used in PET imaging by binding to a positron-emitting metal.  $^{57}\text{Co}$ , which has a half-life of 270 d, has been used with BLM for tumor detection.<sup>15</sup> Furthermore,  $^{55}\text{Co}$  is a cyclotron-produced positron-emitting radionuclide with a half-life of 18.2 h, and it has been used in the detection of lung cancer using a positron camera. Results were compared with those obtained using single photon detection with  $^{55}\text{Co}$ -bleomycin and  $^{57}\text{Co}$ -bleomycin.<sup>16</sup>

One of the best applications of bithiazole-metal complexes is their use in biological activities in mammals. The metal bithiazole complexes reveal the type of DNA rings and target specific areas for cleavage and binding.<sup>17</sup> Both 2,2'-bithiazole and 4,4'-bithiazole have luminescent behaviours depending on whether circulating tumor DNA is present or not. Additionally, they can increase the melting temperature of DNA when binding bleomycin to DNA.<sup>18</sup> Coordination chemistry of bithiazoles also includes those bleomycin species used for medical purposes, as discussed in Section 1.4.1.

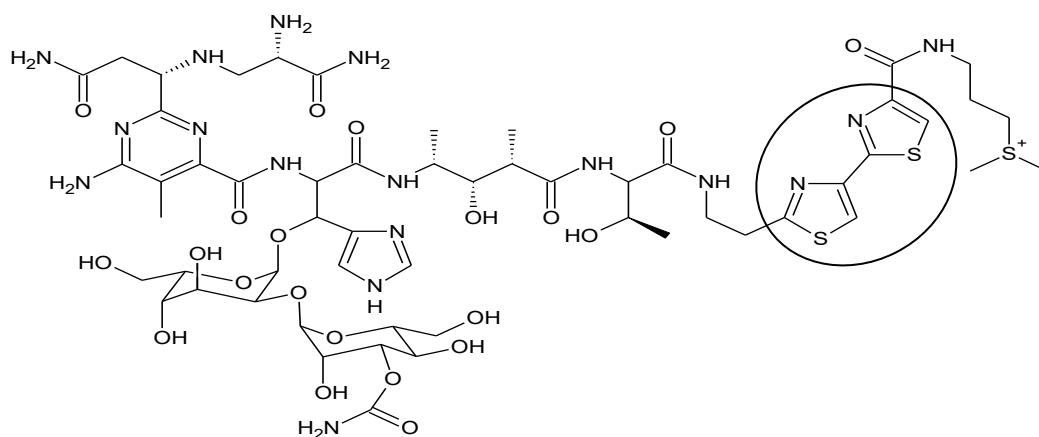


Figure 1.9: Bithiazole domain of bleomycin



### 1.4.2 Materials applications of bithiazole

Semiconducting polymers containing thiazole and bithiazole rings show great potential due to the stability of the ring as compared to some other commonly-used such as building blocks.<sup>19</sup> Researchers are in the process of developing organic electronics using bithiazole based semiconductors as solar cells and photovoltaic sensitizers because of their advantages of being low cost, easy to fabricate, lightweight, and have the capability to fabricate flexible large-area devices.<sup>20</sup>

### 1.4.3 Coordination chemistry of bithiazole

As seen in the previous sections, the bithiazole moiety can be used to bind to metal cations. Bithiazole can be compared to the common organic ligand bipy. The two derivatives of bithiazole, 4-TZ and 2-TZ shown in (Figure 1.7) have similar structures to bipy, so they should share common coordination properties. All the derivatives of bithiazole and bipy could act as bidentate ligands and interact with the metal by chelation effect, forming stable 5-membered metallo heterocycles. The difference in the N-M-N bite angle between bithiazoles and bipy may cause the former to have greater selectivity for specific metals e.g., large or heavy metals such as lead or mercury. In cases where the bite angle is not an issue for making metal complexes, bipy and bithiazole ligands may be interchangeable. In theory, the sulfur atoms could also form a chelate, at least in the 2-TZ isomer,<sup>21</sup> but metal cation-thiophene sulfur interactions are typically weak and usually only occur if the cation and sulfur are forced into close proximity by solid-state packing.

## 1.5 Coordination polymers and metal-organic frameworks

The node-and-spacer method<sup>22-23</sup> of assembling extended coordination structures can be used to create coordination polymers that contain metal cations alternating with bridging ligands. If the structures are extended into three dimensions, the resulting materials are usually called metal-organic frameworks (MOFs). These materials are constructed by joining metal-containing units with organic linkers, using strong bonds. The stability of MOFs can be affected by multiple factors, including the synthetic conditions, metal ions, organic ligands, and metal-ligand coordination geometry. Therefore, the stability of MOFs can be correlated with the strength of the bonds that form the framework. The metal-ligand bond strength determines the thermodynamic stability of MOFs under many environmental conditions.<sup>24</sup>

### 1.5.1 Extended structures using silver(I) with organic nitriles

Silver(I) complexes have been comprehensively prepared by coordinating the metal to N-donor heterocyclic ligands, especially five- and six-membered unsaturated N heterocycles and their derivatives. As a  $d^{10}$  metal cation, Ag(I) has no geometric preference, and so can take in any geometry from linear to octahedral. The chemistry of Ag(I) allows it to form bonds to many different ligand types and can also form metal-metal bonds between two or more Ag(I)-Ag(I) cations.<sup>25</sup>

The silver bond formation with the ligands results in the formation of a coordination polymer. The process is influenced by kinetic factors, and the ability of the coordination polymer to self-assemble. Ag(I) has always maintained a diverse range of functions due to its structure and the coordination polymers formed as a result of the ligand interactions

are either mono- or di-links with the N-donor ligands. When a more flexible ligand is used, such as a pyridyl ligand, it becomes difficult to predict the solid-state structure of the resulting MOF.<sup>26</sup> It has a flexible coordinating sphere that accommodates a range of stable coordination numbers, basically from 2 - 6, in various geometries.<sup>24</sup> On the other hand, when rigid ligands are substituted phenyls, the resulting coordination compounds will have specific stoichiometries based on the ligand's geometry.<sup>27</sup>

## **1.6 General goals of this thesis**

The development of bithiazoles for use in medical materials chemistry will depend on several factors related to the topics covered above. First, we will present synthetic routes to new bithiazole compounds. In our case, we will use these new compounds as ligand for MOFs; however, the methods develop should have wider applicability to any field where bithiazoles are relevant, such as in medical or materials chemistry.

Following ligand preparation, syntheses of coordination compounds will be undertaken. Our goal is to generate MOFs using the nitrile silver(I) supramolecular synthon. We will investigate the solid-state structures by various methods to determine the solids' properties. The observations will be analyzed using the fundamental principles discussed above, e.g. bond strengths from backbonding, coordination geometry from ligand geometry and chelating ability, and colour a based-on ligand field theory. We are interested in MOFs for uses like chemical sensors, e.g. solvent exchange or colorimetric heavy metal detection by chelation. However, we think our results should be transferable to other fields such as generating new bithiazole-containing pharmaceuticals, including those compounds that could carry metals for imaging and therapy.

## Chapter 2

### Ligand Synthesis

#### 2.1 Introduction to 2,2'-bithiazole and 4,4'-bithiazole

The biological activity of bithiazoles and their coordination compounds has given rise to an intense interest in their chemistry. Chelating bithiazoles may have different properties than bipyridyl since the five-member heterocycle will set a greater 'bite' angle to the chelate ring and, in that way, introduce a change to the metal ion environment. The coordination chemistry of these heterocycles is known as they act as bidentate chelating ligands through the two endocyclic nitrogen atoms.<sup>28-29</sup>

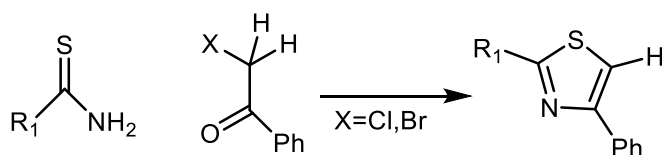
Both 2,2'-bithiazole and 4,4'-bithiazole also have the ability to act as co-formers in coordination compounds. Generally speaking, their ability to act as second-sphere co-former in crystallization processes was established for several coordination compounds of Fe (III). Crystallization of coordination polymers of FeCl<sub>3</sub> with 4,4'-dimethyl-2,2'-bithiazole is greatly facilitated by the presence of the 4,4'-dimethyl-2,2'-bithiazole, even when the bithiazole is not interacting with the metal centre.<sup>30</sup> As well transition metal complexes of bithiazole derivative ligands have found increasing application in extended structures. The 2,2'-bithiazole is found in an interesting class of materials that are of widespread interdisciplinary interest because of the similarity of the structure of thiazole to thiophene, which is the most commonly used as building block for conducting polymers.<sup>31</sup>

Our group has previously synthesized bithiazole ligands containing the 5,5'-dicyano-2,2'-bithiazole core. Several derivatives of this ligand type form a variety of complexes

with silver(I) salts. We want to make the 4,4'-analogue to see if there is any substantive difference between the two ligand systems.

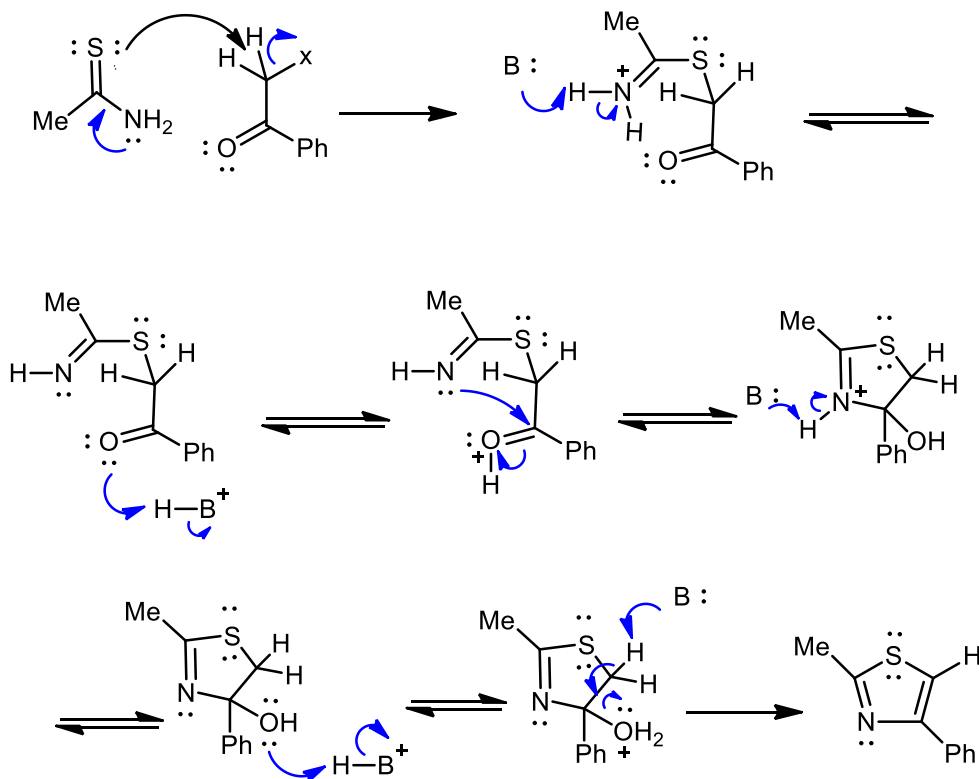
## 2.2 The Hantzsch Thiazole Synthesis

The most common method of generating thiazole is a ring-closing reaction between a thioamide and a 1-halo-2-ketone, as shown in **Scheme 2.1**.



Scheme 2.1: Formation of a Thiazole using the Hantzsch Thiazole Synthesis

The synthesis of 1-halo-2-ketones is well-established, but the compounds tend to be light or heat sensitive and decay over time. Thus, they are best prepared fresh from the ketone. This substrate is attacked by the thioamide in an S<sub>N</sub>2 process which results in an intermediate thiazoline. The thiazoline is then dehydrated, which causes the aromatization of the intermediate while losing a hydrogen halide group. The free hydrogen halide catalyzes the elimination of water to give the thiazole. The entire reaction mechanism<sup>32</sup> is shown in **Scheme 2.2**.



Scheme 2.2: Mechanism of the Hantzsch Thiazole Synthesis

### 2.2.1 Proposed ligand comparison

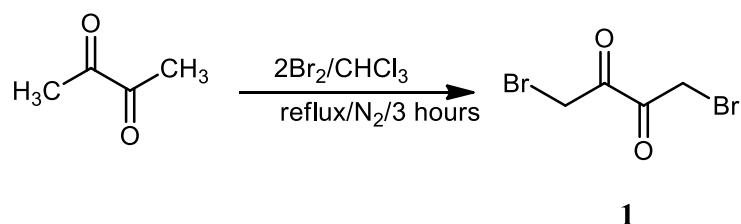
The proposed ligand comparison of the coordination chemistry of the 2,2' and 4,4' isomers of bithiazole has not previously been done. Presumably this is because they have different synthetic routes that are more amenable to different substituent groups (for example, amino is a common substituent for the 4,4'-isomer but it is wholly unknown for the 2,2'-isomer). The position of the sulfur in the ring changes; therefore, the location of the substituents may also change. It has also been noted that 2,2'-bithiazole isomers are more stable than 4,4'-bithiazole since the electron affinity of the former is higher.<sup>33</sup> It can be simply stated that the two synthetic routes tend to give rise to different products (or

that each route is easy for certain substituents, but the substituents are often different between the two isomers). Therefore, it is often hard to find a synthetic route to electronic/steric analogs to directly compare a 2,2'- with a 4,4'-bithiazole ligand.

## 2.3 Synthesis of Ligand Target

### 2.3.1 Synthesis of 1,4-dibromo-2,3-butanedione

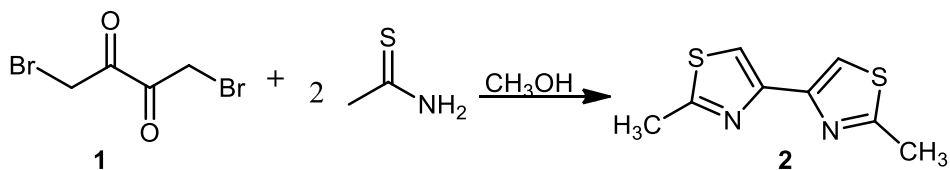
The common synthesis of all 4,4'-bithiazole isomers starts with an (n, n+1)-diketone, the simplest of which we will use is 2,3-butanedione. This compound was prepared adapting a literature preparation involving the bromination of a diketone.<sup>34</sup> This product was characterized using <sup>1</sup>H NMR spectroscopy and was determined to have been synthesized successfully in a very good yield (97%). This product will be used to synthesize all of the proposed 4,4'-bithiazole compounds.



Scheme 2.3: The synthesis of 1,4-dibromo-2,3-butanedione

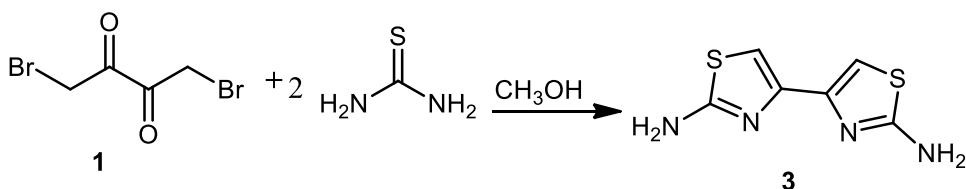
### 2.3.2 Ring-closing Syntheses of 4,4'-Bithiazoles

The dibromobutanedione made above was converted to bithiazole by reaction with a thioamide. The dimethyl derivative **2** was prepared following a literature route<sup>14,35</sup> utilizing the Hantzsch synthesis. The following synthesis proceeded in a good yield (81%). This product was characterized using <sup>1</sup>H NMR spectroscopy.



Scheme 2.4: The synthesis of 2,2'-dimethyl-4,4'-bithiazole

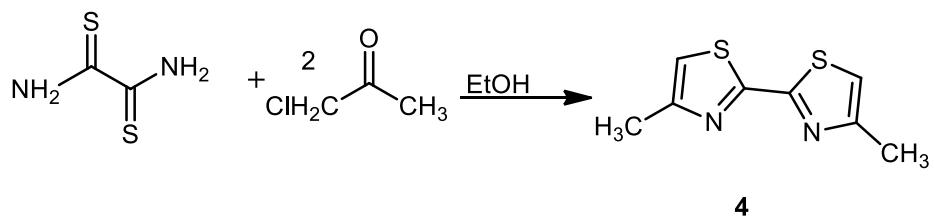
If, instead of thioacetamide, thiourea is used, the diamino derivative **3** is prepared.<sup>36</sup> The synthesis proceeded in a good yield (83%). This product was characterized using <sup>1</sup>H NMR spectroscopy.



Scheme 2.5: The synthesis of 2,2'-diamino-4,4'-bithiazole

### 2.3.3 Ring-closing Syntheses of 2,2'-Bithiazole

The 2,2'-bithiazole was prepared following a literature route<sup>37</sup> utilizing the Hantzsch synthesis. The following synthesis **4** proceeded in a good yield (82%). This product was characterized using <sup>1</sup>H NMR spectroscopy.

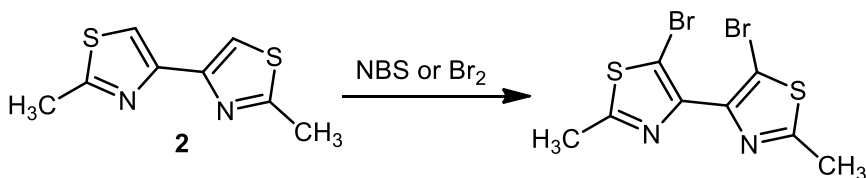


Scheme 2.6: The synthesis of 4,4'-dimethyl-2,2'-bithiazole



### 2.3.4 Synthesis of Dicyanobithiazoles

There are a number of methods for attaching nitrile groups to an aromatic ring. One method is the substitution of a halogen with a nitrile using copper(I) cyanide (the Rosamund-von Braun reaction).<sup>38</sup> Therefore, the halobithiazoles needed to be prepared for the subsequent coupling reactions to proceed. Compound **2** was chosen for the initial attempts since it has only one aromatic proton, and an inert substituent on the other carbon. Multiple conditions were used to test various halogenation options. Both N-bromosuccinimide (NBS) and elemental bromine were used as halogenating sources. The latter was performed in chloroform and led to a moderate yield (64%). Bromination with NBS was attempted in several solvents: THF, DMF, and a 1:1 mixture of chloroform and glacial acetic acid (GAA). This last solvent mixture performed poorly with only 29% yield; however, the other solvents gave good yields (73-98%). This product was characterized using <sup>1</sup>H NMR spectroscopy. The mass spectrum shows an (M+1)<sup>+</sup> peak that shows the correct isotopic pattern for a dibromo species.

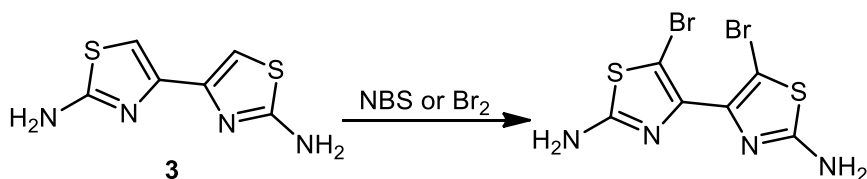


Solvents conditions: THF, DMF, CHCl<sub>3</sub>/GAA (1:1), or CHCl<sub>3</sub>

Scheme 2.7: Bromination of 2,2'-dimethyl-4,4'-bithiazole

Similarly, halogenation of the substrate **3** was attempted under several sets of conditions. The first method was conducted using NBS, chloroform and glacial acetic acid; the second method used NBS, N, N-dimethylformamide and glacial acetic acid. Both

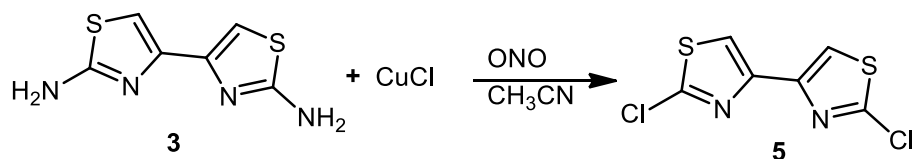
sets of reaction conditions were unsuccessful resulting in a very low yield. On the other hand, the reaction that used NBS and N, N-dimethylformamide only as a solvent, produced a good yield (74%). Halogenation using elemental bromine with chloroform solvent also gave rise to a successful reaction with good yield (86%). In the mass spectrum, we see multiple peaks, but one peak that we can find the molecule at 353 (M+1)<sup>+</sup>.



Solvents conditions: DMF, CHCl<sub>3</sub>/GAA (1:1), or CHCl<sub>3</sub>

Scheme 2.8: Bromination of 2,2'-diamino-4,4'-bithiazole

Another route to cyano-substituted aromatics is through the Sandmeyer reaction, exchanging an amine for a halide. In this case, the Sandmeyer reaction was used to substitute an amine group by a chloro group. Using copper (I) chloride gave the best results in the reaction. As shown in **Scheme 2.9**, the product was successfully synthesized in sufficient yields of approximately (58.8%), and this product was characterized using <sup>1</sup>H and <sup>13</sup>C NMR spectroscopy. Unfortunately, the mass spectrum shows a large number of extra peaks at larger *m/z* values and it was not possible to detect the parent peak.

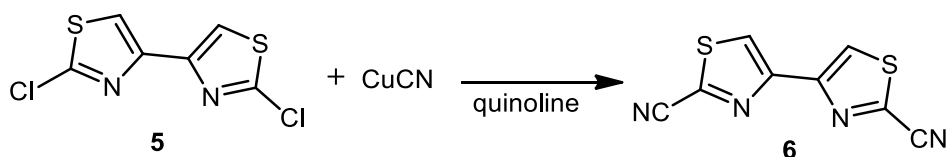


Scheme 2.9: Deamination of 2,2'-dichloro-4,4'-bithiazole

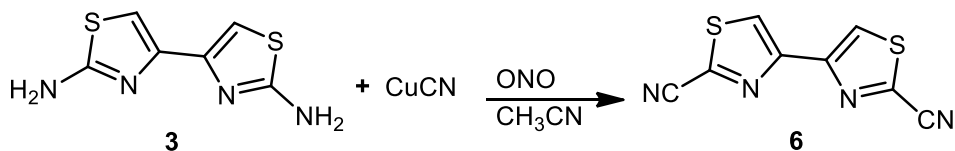
Conversion of the various halides to nitriles using Rosamund-von Braun conditions was then attempted. Both quinoline and N, N-dimethylformamide (DMF) were used as solvents. The two solvents have quite different boiling points (the reaction is performed in refluxing solvent). The better result came from quinoline with a crude yield (after filtration and removal of water-soluble biproducts) of 93%, as shown in **Scheme 2.10**. From IR spectroscopy, the presence of an aromatic nitrile group was confirmed at 2134 cm<sup>-1</sup>. It assumes that there is only one product because the nitrile peak is quite sharp and is a single peak.

The direct conversion of the amine to a nitrile under Sandmeyer conditions is another possible route, at least for an amino-substituted bithiazole, i.e. the reaction of 2,2'-diamino-4,4'-bithiazole with tert-butyl nitrite and dry acetonitrile as solvent and copper(I) cyanide as the nitrile source. The presence of the aromatic cyano groups was confirmed by IR spectroscopy, showing two peaks in the nitrile range at 2169 and 2123 cm<sup>-1</sup> respectively. This implies multiple products, neither of which are the same as the product from the quinoline reaction. There are a number of possibilities, among them incomplete reaction (e.g. generating a nitrile/amino) or cases with protonation on either the basic ring or remaining amino nitrogen. Although the IR and mass spectral results are promising to show a CN stretch and the molecular ion at 219 (M+1)<sup>+</sup> amu, purification has proven to be difficult. The IR data suggests two distinct nitrile species that we have been unable to

separate by column chromatography or fractional sublimation. The mass spectrum does contain a peak at 254 amu, which is consistent with the bis(amide) i.e. the hydrolysis product of the dinitrile and water. This has been seen before in the Mackinnon group where the nitriles become activated and hydrolyzed in the workup.



Scheme 2.10: Cyanation of 2,2'-dichloro-4,4'-bithiazole



Scheme 2.11: Cyanation of 2,2'-diamino-4,4'-bithiazole

## 2.4 Conclusion

1,4-dibromo-2,3-butanedione was successfully synthesized and used to prepare both 2,2'-dimethyl-4,4'-bithiazole and 2,2'-diamino-4,4'-bithiazole. Conversion of these ring systems to nitriles has been accomplished, on the evidence of IR spectroscopy, by the conversion of a chlorobithiazole and an aminobithiazole to nitriles. Purification was difficult perhaps due to the basic nature of the thiazole ring nitrogens, which might become protonated. Unfortunately, the need to maintain basic conditions to avoid protonating the ring nitrogens may render these synthetic routes untenable, since organic nitriles are easily hydrolyzed in basic conditions. Other routes to aromatic nitriles may be discovered to be better than the routes presented here and will be investigated in the future.

## 2.5 Experimental

### 2.5.1 Instrumentation

Nuclear magnetic resonance (NMR) spectra were recorded on a Varian Unity Inova (500 MHz) spectrometer at the Lakehead University Instrument Laboratory (LUIL). All chemical shifts are reported at room temperature in parts per million (ppm) referenced to tetramethylsilane (TMS) added internally to the solvent.  $^1\text{H}$  NMR spectra were obtained by dissolving the substance in  $\text{CDCl}_3$  or  $(\text{CD}_3)_2\text{SO}$ . Infrared spectra (IR) were obtained as nujol mulls (solids) or neat thin films (liquids) on sodium chloride plates on an IBM IR/32 FT-IR spectrophotometer, peaks are reported in wave numbers ( $\text{cm}^{-1}$ ) and are uncalibrated.

## 2.5.2 General Synthesis

Fine chemicals were obtained from commercial sources and used as received, unless otherwise stated. Solvents were purified before use by standard methods,<sup>39</sup> and reactions were carried out under an atmosphere of dry N<sub>2</sub>. The following compounds were synthesized by the literature routes: 1,4-dibromo-2,3-butanedione,<sup>34</sup> 2,2'-dimethyl-4,4'-bithiazole,<sup>14,35</sup> and 2,2'-diamino-4,4'-bithiazole,<sup>36</sup> the identity of these synthesized chemicals was verified using <sup>1</sup>H and <sup>13</sup>C NMR. For more details see appendix.

## 2.5.3 Preparation of 2,2'-dichloro-4,4'-bithiazole (5)

Copper (I) chloride (2.26g, 16.80 mmol) and tert-butyl nitrite (1.06g, 10.27 mmol) were added to an oven-dried 500mL 3-necked round-bottom flask equipped with a gas nozzle, stir bar, thermometer, and rubber septum. The flask was evacuated and filled with N<sub>2</sub>. Dry acetonitrile (40mL) was added via syringe. The solution was heated to 65 °C and 2,2'-diamino-4,4'-bithiazole (1.00g, 5.04 mmol) was added portion-wise over the course of 15 min, with constant stirring. The resulting mixture was refluxed for two hours. The reaction was mixed with 20%HCl (80 mL) and extracted with diethyl ether (3×50mL). The combined organic phases were washed with 20%HCl (80mL) and extracted with diethyl ether (50 mL) and dried over MgSO<sub>4</sub>. The solvent was removed via rotary evaporation to yield a brown solid (0.70g, 58.8%). <sup>1</sup>H NMR (500 MHz, chloroform-*d*): δ 7.68 (s, 1H). <sup>13</sup>C NMR (126 MHz, chloroform-*d*): δ 117.49, 148.09, 152.50. IR (nujol mull): 3126 (m), 3102 (w), 1260 (w), 1048 (s), 772 (w), 747 (m) cm<sup>-1</sup>.

## 2.5.4 Preparation of 2,2'-dicyano-4,4'-bithiazole

### (a) Rosamund-von Braun route

2,2'-dichloro-4,4'-bithiazole (1.56g, 6.57mmol) and copper(I) cyanide (1.11g, 12.39 mmol) were added to an oven-dried 300mL 3-necked round-bottom flask equipped with a gas nozzle and stir bar. The flask was flushed with N<sub>2</sub> and heated to 70 °C. Dry quinoline (50mL) was added via syringe. The mixture was refluxed over three hours and the resulting mixture cooled to room temperature until not boiling. The mixture was transferred to a one-liter beaker containing 350mL ice +50mL HCl. Once the ice melted, a light brown solid was isolated, washed with distilled water and cold ethanol. IR (nujol mull): 2134 (w), 1461 (s), 1377 (m), 1302 (w), 813 (m), 768 (m) cm<sup>-1</sup>. Mass spec. calc. For C<sub>8</sub>H<sub>2</sub>N<sub>4</sub>S<sub>2</sub>: 218.0, found 218.9 (M+1)<sup>+</sup>, 253.9 (M+2H<sub>2</sub>O)<sup>+</sup>.

### (a) Sandmeyer route

copper(I) cyanide (2.28g, 16.95 mmol) and tert-butyl nitrite (1.03g, 9.98mmol) were added to an oven-dried 500 mL 3-necked round-bottom flask equipped with a gas nozzle, stir bar, thermometer, and rubber septum. The flask was evacuated and filled with N<sub>2</sub>. Dry acetonitrile (40mL) was added via syringe. The solution was heated to 65 °C and 2,2'-diamino-4,4'-bithiazole (1.00g, 5.04 mmol) was added as solid portion-wise in five-minute intervals while the mixture was stirring. The resulting mixture was refluxed for 2 hours, the mixture was concentrated on a rotary evaporator then 50 mL of distilled water was added, and the mixture filtered the mixture yields a black solid (0.39g, 35%). IR (nujol mull): 2169 (m), 2123 (w), 1616 (m), 1533 (m), 1456 (s), 1377 (m) cm<sup>-1</sup>. Mass spec. calc. For C<sub>8</sub>H<sub>2</sub>N<sub>4</sub>S<sub>2</sub>: 218.0, found 218.9 (M+1)<sup>+</sup>, 253.9 (M+2H<sub>2</sub>O)<sup>+</sup>.

### 2.5.5 Preparation of 5,5'-dibromo-2,2'-dimethyl-4,4'-bithiazole

To a flat bottom flask equipped with a stir bar was added 2,2'-dimethyl-4,4'-bithiazole (1.00g, 5.09mmol), and THF (50ml). To this solution, NBS (2.88g, 16.18mmol) was added scoop-wise over the course of 10 min. Light was excluded by stirring the reaction covered by a dark box. The mixture was allowed to stir in the dark overnight. The next day, 100mL of distilled water was added to the mixture, followed by extraction with diethyl ether (3×50mL) and dried over MgSO<sub>4</sub>. The solvent was evaporated via rotary evaporation to yield an orange solid (1.78g 98%). <sup>1</sup>H NMR (500 MHz, chloroform-d): δ 2.78 (s, 3H). <sup>13</sup>C NMR (126 MHz, chloroform-d): δ 19.65, 107.90, 145.80, 166.95. IR (nujol mull): 1792 (w), 1596 (w), 1198 (w), 1173 (s), 1008 (m), 907 (m) cm<sup>-1</sup>. Mass spec. calc. For C<sub>8</sub>H<sub>6</sub>N<sub>2</sub>S<sub>2</sub><sup>79</sup>Br<sub>2</sub>: 353.8. found 354.8 (M+1)<sup>+</sup> 376.8 (M+Na)<sup>+</sup>.

### 2.5.6 Preparation of 5,5'-dibromo-2,2'-diamino-4,4'-bithiazole

To a flat bottom flask equipped with a stir bar was added 2,2'-diamino-4,4'-bithiazole (1.00g, 5.04mmol), and DMF (50ml). In this solution, NBS (2.50g, 14.04mmol) was added scoop-wise over the course of 10 min. Light was excluded by stirring the reaction covered by a dark box. The mixture was allowed to stir in the dark overnight. The next day, 100 mL of distilled water was added, and the mixture was filtered and yielded a black solid (1.34g 74%). <sup>1</sup>H NMR (500 MHz, chloroform-d): δ 1.67 (s, 4H). IR (nujol mull): 1700 (w), 1655 (m), 1523 (w), 1105 (m) cm<sup>-1</sup>. Mass spec. calc. For C<sub>6</sub>H<sub>4</sub>N<sub>4</sub>S<sub>2</sub><sup>79</sup>Br<sub>2</sub>: 353.8. Found 353.0 (M-1)<sup>+</sup>.

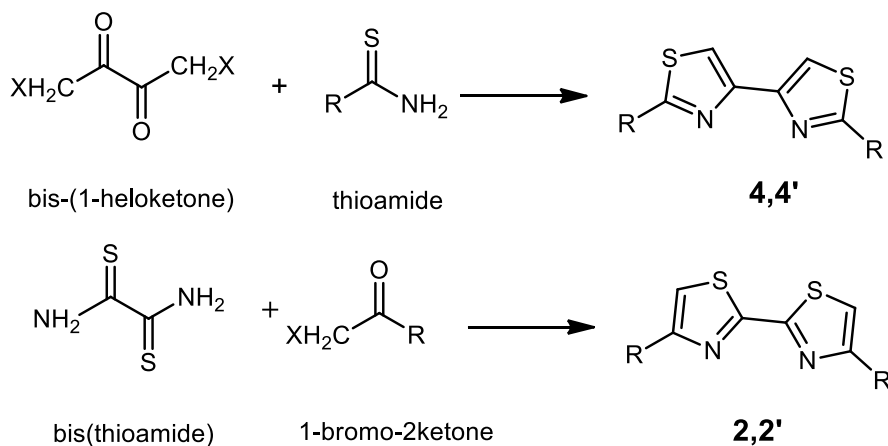


## Chapter 3

### Comparison of Bithiazole Regioisomers as Ligands

#### 3. 1 Introduction to a systematic comparison of 4,4' vs 2,2' with metals

Two bithiazoles that contain a bipy-like core are the 2,2'- and the 4,4'-bithiazole isomers. The synthesis of both utilizes the Hantzsch method, where the 2,2'-isomer is made from an  $n, n+1$ -bis(thioamide) while the 4,4'-isomer comes from an  $n, n+1$ -diketone. The reaction conditions are similarly equivalent – usually reaction in refluxing dry methanol or ethanol. Alkyl substituents can be incorporated into both isomers by including a group on the complementary piece – an alkylketone adding to the bis(thioamide) for an alkylated 2,2'-isomer, or an alkylthioamide added to the diketone for an alkylated 4,4'-isomer. Isolation and purification under ambient conditions is usually facile, such as recrystallization from benzene-acetonitrile.<sup>28</sup>



Scheme 3.1: Synthesis of bithiazoles

Derivatization of both 2,2' and 4,4' isomers is possible through electrophilic aromatic substitution of the aromatic rings. The rings are activated because of the electron density from the heteroatoms in the ring. This enhanced electron density is provided to the position's alpha to the heteroatoms with this being the main site of substitution (therefore, the sites of substitution on the two bithiazoles will be different). It appears that the site  $\alpha$  to the sulfur is preferred, although in the case of alkyl bithiazoles, which have only one aromatic hydrogen there is no need to consider regioselectivity. These different isomers will necessarily lead to different coordination compounds, even if they are both *N, N*-chelating.



Scheme 3.2: The bithiazole binds as an *N, N*-chelate with metal

Different metals bind to bithiazole in different ways. Environmentally problematic cations such as  $\text{Pb}^{2+}$ ,  $\text{Zn}^{2+}$ ,  $\text{Cd}^{2+}$ ,  $\text{Cu}^{+2}$ ,  $\text{Hg}^{+2}$  among others have been shown to bind to 4,4'-bithiazole derivatives.<sup>40</sup> In all these cases, the bithiazole binds as an *N, N*-chelate, and the rings are forced into a nearly co-planar orientation. In solution, they deviate significantly from planarity - analyses have indicated that there is a series of rotamers in solution.<sup>41</sup>

Therefore, in an attempt to screen which metal cations will bind with bithiazole, we turned to UV-visible absorbance spectroscopy. If a ligand binds to a metal in solution at any reasonable strength for any reasonable amount of time (has a large enough

equilibrium constant), the  $\lambda_{\max}$  of the ligand should shift because of the interaction. The donation of a lone pair from aromatic heterocycle to the metal creates a more positive charge on the N-atom; changing the orbital energies in the  $\pi$ -system, which in turn changes the  $\lambda_{\max}$ .

### **3.2 Attempted characterization of bithiazole coordination compounds in solution**

We chose to look at two similar ligands and investigate their relative interactions with a series of metal cations. The methylated ligands chosen were 5,5'-dimethyl-2,2'-bipyridyl (Me-bipy) and 2,2'-dimethyl-4,4'-bithiazole (Me-4Tz). Metal salts were dissolved in water. The best solvent in which to dissolve the ligands was found to be acetonitrile, which balanced the need for miscibility in water with solubility of the ligand. Ethanol also meets these requirements, but has a longer wavelength cutoff, which can obscure the ligand absorption. In none of the reported results was there evidence (naked eye or UV-vis noise caused by scattering) of precipitation when the two solutions were mixed.

The metal salts were mixed in a 1:1 ratio with the ligand being tested. These solutions were analyzed using UV-Vis spectroscopy and the spectra were compared to the spectra of the ligand without metal salts. Based on a conjugation argument where the M-d-orbital participates in the chelate  $\pi$ -system, it would expect an increase in the  $\lambda_{\max}$  corresponding to the increased amount of  $\pi$ - conjugation in the coordination compound.

### 3.2.1 Testing of ligand-metal solutions in acetonitrile and ethanol

The uncoordinated Me-bipy ligand has an absorption peak at 280.0 nm. The ligand-metal solutions were tested, and the peaks were compared with the ligand peak. Those that showed a difference in the position of peaks were determined to have a bound metal-ligand complex.

To determine if there is a solvent affect, these same six cations that successfully coordinated to Me-bipy were tested in acetonitrile solutions. For Me-bipy in ethanol, the UV-Vis spectrum determined to be 269.0 nm. The ligand-metal solutions were tested, and the peaks were compared with the ligand peak.

**Table 3.1:** The UV-Vis peaks of the ligand-metal solutions in acetonitrile and ethanol using Me-bipy as ligand in a 1:1 ratio (compared to 280.0 nm, 269.0 nm).

<b>Metal Ion</b>	<b>UV-Vis Peak (nm) CH<sub>3</sub>CN</b>	<b>Change in CH<sub>3</sub>CN</b>	<b>UV-Vis Peak (nm) EtOH</b>	<b>Change in EtOH</b>
Me-bipy only (no metal)	280.0	---	269.0	---
Al <sup>3+</sup>	320.0	40.0	269.0	---
Cr <sup>3+</sup>	320.0	40.0	269.0	---
Ni <sup>2+</sup>	317.0	37.0	299.0	30.0
Y <sup>3+</sup>	315.0	35.0	269.0	---
Cd <sup>2+</sup>	310.0	30.0	292.0	23.0
Pb <sup>2+</sup>	296.5	16.5	269.0	---

As seen in UV-Vis spectra, there were six metal ions that bound with the Me-bipy ligand:  $\text{Al}^{3+}$ ,  $\text{Cr}^{3+}$ ,  $\text{Ni}^{2+}$ ,  $\text{Y}^{3+}$ ,  $\text{Cd}^{2+}$ , and,  $\text{Pb}^{2+}$ . Other metal plus ligand combinations were also tested that did not give any result, i.e., with  $\text{Mg}^{2+}$ ,  $\text{K}^+$ ,  $\text{Ca}^{2+}$ ,  $\text{Cs}^+$ ,  $\text{Ba}^{2+}$ ,  $\text{La}^{3+}$ ,  $\text{Eu}^{3+}$ , and,  $\text{Hg}^{2+}$ .

The data in this table also show a definite solvent effect, with only two of the six cations binding in ethanol. As we see their peaks were significantly shifted from 269.0nm ( $\text{Ni}^{2+}$  at 299.0nm and  $\text{Cd}^{2+}$  at 292.0nm). Unlike the situation observed for reactions between silver(I) and dicyanobithiophene ligand, where binding was observed in all solvents except acetonitrile,<sup>42</sup> the reverse situation seems to be the case here with the acetonitrile being the preferred solvent to see coordination.

In the same way, Me-4-Tz was tested with the same six cations in acetonitrile and ethanol. For the Me-4-Tz in ethanol, the ligand peak was at 262.0 nm and in acetonitrile, the ligand peak was at 262.5 nm. The ligand-metal solutions were tested, and the  $\lambda_{\text{max}}$  compared that of ligand.

**Table 3.2:** The UV-Vis peaks of the ligand-metal solutions in acetonitrile and ethanol using Me-4-Tz as ligand in a 1:1 ratio.

Metal Ion	UV-Vis Peak (nm) $\text{CH}_3\text{CN}$	change in $\text{CH}_3\text{CN}$	UV-Vis Peak (nm) EtOH	change in EtOH
Me-4-Tz only (no metal)	262.0	---	262.0	---
$\text{Al}^{3+}$	262.5	---	262.0	---
$\text{Cr}^{3+}$	262.5	---	262.0	---
$\text{Ni}^{2+}$	257.2	---	262.0	---

Y <sup>3+</sup>	262.5	---	262.0	---
Cd <sup>2+</sup>	262.0	---	262.0	---
Pb <sup>2+</sup>	261.5	---	262.0	---

Looking at the data obtained from the spectra of Me-4-Tz in acetonitrile with the metals, we can determine that the ligand did not bind with any of the six metals. The peaks were all extremely close to the ligand peak of 262.5 nm, although there are some small differences in maximum absorbance (as chosen by the instrument software's peak picker), the differences are not large enough to be significant based on the resolution of the spectrometer. The results of these show that ethanol is no better than acetonitrile for bithiazole ligands with these metal salts.

### 3.3 Isolation of Methylbithiazole Complexes

The above results show that under low concentration conditions, bithiazoles were not observed to form complexes in solution with the various metal cations tested. On the other hand, it is known that bithiazoles do form solid coordination compounds when isolated from solution reactions. For example, Zn (II)<sup>43</sup> and Pb (II)<sup>44</sup> are known to form coordination compounds in the solid state with 4,4'-bithiazole ligands, even though they show no apparent reaction in our absorption screening experiments. Therefore, several large-scale reactions were performed to isolate solid products to determine binding capability of bithiazoles.

### 3.3.1 Synthesis of Methylbithiazole Complexes

Larger-scale reactions were performed using 2,2'-dimethyl-4,4'-bithiazole as ligand. Approximately 0.23 g of the ligand was mixed in a 1:1 ratio of ligand: metal cation. We used cations that have been shown to form coordination compounds with other bithiazole ligands and chose sulfate as the counterion because it is commonly used in solved crystal structures of bithiazole coordination compounds. The reagents were added to a Schlenk tube with dry methanol and heated to reflux for a time ranging from a couple of hours to a couple of days. The solutions were cooled and filtered and the solid collected. The solid was isolated and purified by washing the filtered solid. The isolated solids were then characterized by combustion analysis.

### 3.3.2 Result and discussion

Results are summarized in **Table 3.3**. In all cases, a solid was isolated, usually brightly coloured or at least a different colour than the starting material salt, indicating a change in the coordination sphere of the metal. Because the compounds were not rigorously purified, larger errors in the combustion analyses are to be expected. However, in most cases, a coordination compound can be confirmed by the relative abundancies of nitrogen and sulfur. Only the ligand contains nitrogen, so the ligand must be present in cases where there is nitrogen in the combustion analysis. There is sulfur in both the ligand and the salt (sulfate anion), but the ratio of N:S will necessarily be smaller in the coordination compound than it would be in the ligand itself.

The colour changes observed and the increase in the relative amount of sulfur indicate that the metal salt is also present in the solid. The change in colour suggests

there is a more intimate interaction between the cation and the ligand than mere co-crystallization. Suggested coordination compound stoichiometries consistent with the combustion data are given for each compound in the last column of **Table 3.3**.

**Table 3.3:** Combustion analysis results of 2,2'-dimethyl-4,4'-bithiazole ligand with different salt.

Salt	Solvent	atomic stoichiometries	Ratio ligand:metal:solvent
NiSO <sub>4</sub> ·6H <sub>2</sub> O (blue-green)	C <sub>2</sub> H <sub>5</sub> OH	C <sub>9</sub> H <sub>11</sub> N <sub>2</sub> NiO <sub>4.5</sub> S <sub>3</sub>	1:1:0.5 (gray)
NiSO <sub>4</sub> ·6H <sub>2</sub> O (blue-green)	CH <sub>3</sub> OH	C <sub>8</sub> H <sub>8</sub> N <sub>2</sub> NiO <sub>4</sub> S <sub>3</sub>	1:1:0 (gray)
CoSO <sub>4</sub> ·7H <sub>2</sub> O (pink)	CH <sub>3</sub> OH	C <sub>8</sub> H <sub>8</sub> N <sub>2</sub> CoO <sub>4</sub> S <sub>3</sub>	1:1:0 (pink)
FeSO <sub>4</sub> ·7H <sub>2</sub> O (light green)	C <sub>2</sub> H <sub>5</sub> OH	C <sub>8</sub> H <sub>8</sub> N <sub>2</sub> Fe <sub>4</sub> S <sub>6</sub> O <sub>16</sub>	1:4:0 (light brown)
Fe <sub>2</sub> (SO <sub>4</sub> ) <sub>3</sub> (beige)	CH <sub>3</sub> OH	C <sub>72</sub> H <sub>72</sub> N <sub>18</sub> Fe <sub>3</sub> S <sub>20</sub> O <sub>8</sub>	No reaction (light brown)
YCl <sub>3</sub> (white)	CH <sub>3</sub> OH	C <sub>32</sub> H <sub>32</sub> N <sub>12</sub> S <sub>12</sub> YC <sub>l3</sub>	No reaction (light brown)
MnSO <sub>4</sub> ·H <sub>2</sub> O (pale pink)	CH <sub>3</sub> OH	C <sub>8</sub> H <sub>8</sub> N <sub>2</sub> Mn <sub>4</sub> S <sub>6</sub> O <sub>16</sub>	1:4:0 (light brown)
CuSO <sub>4</sub> ·5H <sub>2</sub> O (blue)	CH <sub>3</sub> OH	C <sub>8</sub> H <sub>8</sub> N <sub>2</sub> CuO <sub>4</sub> S <sub>3</sub>	1:1:0 (light blue)

Although there is no binding to any tested metal cation in dilute solution, these isolated solids do appear to be coordination compounds. For example, the two isolated Ni<sup>2+</sup> species analyze to approximately Ni<sup>2+</sup>: L ratio 1:1, whereas there is no shift in the solution UV-Visible absorption peak. This indicates that, at least for these ligand-cation systems,



UV-Visible absorption cannot be used as a screening experiment to determine what cations are likely to bind to bithiazole ligand.

In fact, binding seems to be general for cations in the first transition series, at least for the  $M^{2+}$  oxidation state, since all of  $Mn^{2+}$ ,  $Fe^{2+}$ ,  $Ni^{2+}$ , and  $Cu^{2+}$  appear to give coordination compounds when isolated from solution.

## **3.4 Experimental**

### **3.4.1 General considerations**

Chemicals were reagent grade purchased from commercial sources and used as received unless otherwise stated Me-4-Tz was synthesized as described in section 2.3.2. All UV-visible absorption spectroscopy was obtained using an Agilent Technologies Cary 60 UV-Vis spectrometer. Combustion analysis was acquired using the Elementar Vario EL Cube analyzer for elemental analysis C, H, N and S in the Lakehead University Instrumentation Laboratory (LUIL).

### **3.4.2 UV-visible absorption experiments**

Metal salts were dissolved in 100 mL of water to give solution concentrations of 0.003 M. The following metal solutions were made: Aluminum (III) nitrate (0.1130 g, 0.0003 mol), Chromium (III) nitrate (0.1196 g, 0.0003 mol), Nickel (II) chloride (0.0719 g, 0.0003 mol) Yttrium (III) chloride (0.0940 g, 0.0003 mol), Cadmium (II) chloride (0.0687 g, 0.0003 mol) Lead (II) nitrate (0.0990 g, 0.0003 mol).

In order to prepare the ligands for testing, the following ligands were used: dimethyl-bipy (0.0549 g, 0.0003 mol) and Me-4-Tz (0.0588 g, 0.0003 mol). Each solution was made

in a 100 mL volumetric flask, giving a concentration of 0.003 M in either ethanol or acetonitrile. Each ligand was tested in both solvents to determine which is the best solvent. Acetonitrile was used because of its large range in UV-Vis spectroscopy.

The following procedure was used to prepare the solutions for testing: 1 mL of the 0.003 M ligand solution was added to a volumetric flask. 1 mL of the 0.003 M metal solution was added to the volumetric flask, and then diluted to 100 mL with ethanol or acetonitrile. Each was examined using UV-Vis spectroscopy.

### **3.4.3 Isolation of bithiazole-metal complexes**

#### **3.4.3.1 Me-4-Tz with NiSO<sub>4</sub>•6H<sub>2</sub>O**

Method 1 (in methanol): NiSO<sub>4</sub>•6H<sub>2</sub>O (0.1403 g 0.0009 mol) was added to a Schlenk tube. 20 mL of anhydrous methanol was added to a flask and the contents were dissolved to give a blue solution, and Me-4-Tz (0.1955 g 0.0001 mol) was added to the flask. The mixture was left to reflux under nitrogen gas with heating for 1h. The product was isolated by the suction filtration of solution to give a gray solid. Product analysis for L•NiSO<sub>4</sub>; Analysis. Calcd. for C<sub>8</sub>H<sub>8</sub>N<sub>2</sub>NiO<sub>4</sub>S<sub>3</sub>: C 27.37, H 2.30, N 7.98, S 27.40 %. Found: C 24.74, H 2.91, N 7.00, S 23.58 %.

Method 2 (in ethanol): NiSO<sub>4</sub>•6H<sub>2</sub>O (0.1536 g 0.0001 mol) was added to a Schlenk tube. 20 mL of anhydrous ethanol was added to a flask and the contents were dissolved. Me-4-Tz (0.2296 g 0.0011 mol) was added to the tube and refluxed for 72 hours. Once the solution had cooled to room temperature, 20 mL of acetone was added. This was followed by suction filtration to isolate the product a gray solid. Product analyses for L•NiSO<sub>4</sub>.0.5 EtOH; Analysis. Calcd. for C<sub>9</sub>H<sub>11</sub>N<sub>2</sub>NiO<sub>4.5</sub>S<sub>3</sub>: C 29.53, H 3.03, N 7.65, S 26.28 %. Found: C 28.97, H 3.38, N 8.36, S 25.26 %.

### 3.4.3.2 Me-4Tz with $\text{CoSO}_4 \cdot 7\text{H}_2\text{O}$

$\text{CoSO}_4 \cdot 7\text{H}_2\text{O}$  (0.1422 g 0.0005 mol) was added to a Schlenk tube, and 20 mL of anhydrous methanol was added to a flask and the contents were dissolved resulting in a pink solution. Me-4-Tz (0.1955 g 0.0001 mol) was added to the flask. The mixture was left to reflux under nitrogen gas with heating for 1h. This was followed by suction filtration of the solution to give a pink solid. Product analysis shows  $\text{L} \cdot \text{CoSO}_4$ ; Analysis. Calcd. for  $\text{C}_8\text{H}_8\text{N}_2\text{CoO}_4\text{S}_3$ : C 27.35, H 2.30, N 7.97, S 27.38 %. Found: C 22.96, H 2.90, N 6.56, S 22.77 %.

### 3.4.3.3 Me-4Tz with $\text{FeSO}_4 \cdot 7\text{H}_2\text{O}$

$\text{FeSO}_4 \cdot 7\text{H}_2\text{O}$  (0.1488 g 0.0005 mol) was added to a Schlenk tube. 20 mL of anhydrous ethanol was added to a flask and the contents were dissolved. Me-4-Tz (0.2296 g 0.0011 mol) was added to the tube, and it was left to reflux for 72h. The solution was cooled to room temperature, 20 mL of acetone was added to the solution. This was followed by the suction filtration a light brown solid was obtained from the Iron solution. Product analyses for  $\text{L} \cdot (\text{FeSO}_4)_4$ ; Analysis. Calcd. for  $\text{C}_8\text{H}_8\text{N}_2\text{Fe}_4\text{S}_6\text{O}_{16}$ : C 11.95, H 1.00, N 3.48, S 23.93 %. Found: C 12.61, H 1.29, N 3.36, S 21.36 %.

### 3.4.3.4 Me-4-Tz with $\text{Fe}_2(\text{SO}_4)_3$

$\text{Fe}_2(\text{SO}_4)_3$  (0.5098 g 0.0012 mol) was added to a Schlenk tube. Me-4-Tz (0.4989 g 0.0025 mol) was added in the same tube. Anhydrous methanol (13 mL) was added to the flask and the contents dissolved. The mixture was left to reflux under nitrogen gas with heating for 1h. The solution was cooled to room temperature, filtered by the suction filtration to give a light brown solid, from the Iron solution. Product analyses for  $\text{L} \cdot$

$\text{Fe}_2(\text{SO}_4)_3$ ; Analysis. Calcd. for  $\text{C}_{72}\text{H}_{72}\text{N}_{18}\text{Fe}_3\text{S}_{20}\text{O}_8$ : C 40.67, H 3.41, N 11.86, S 30.16 %. Found: C 48.95, H 4.11, N 14.27, S 32.67 %. This is consistent with ligand only with no metal coordination.

#### **3.4.3.5 Me-4-Tz with $\text{YCl}_3$**

$\text{YCl}_3$  (0.5024 g 0.0025 mol) and Me-4-Tz (0.5136 g 0.0026 mol) were added in a Schlenk tube. Anhydrous methanol (13 mL) was added to the flask and the contents dissolved. The mixture was left to reflux under nitrogen gas with heating for 1h. After cooling to room temperature, the solution was filtered to give a light brown solid. Product analyses indicates only Analysis. Calcd for L.  $\text{C}_8\text{H}_8\text{N}_2\text{S}_2$ : C 48.95, H 4.11, N 14.27, S 32.67 % Found: C 48.42, H 3.48, N 14.14, S 32.78 %. This is consistent with ligand only with no metal coordination.

#### **3.4.3.6 Me-4-Tz with $\text{MnSO}_4 \cdot \text{H}_2\text{O}$**

$\text{MnSO}_4 \cdot \text{H}_2\text{O}$  (0.5032 g 0.0033 mol) was added to a Schlenk tube. Me-4-Tz (0.5072 g 0.0025 mol) was added in the same Schlenk tube. Anhydrous methanol (13 mL) was added to a flask and the contents dissolved. The mixture was left to reflux under nitrogen gas with heating for 1h. The solution was cooled to room temperature and filtered to give a light brown solid. Product analyses to approximately  $\text{L} \cdot (\text{MnSO}_4)_2$ ; Analyses. Calc. for  $\text{C}_8\text{H}_8\text{N}_2\text{Mn}_4\text{S}_6\text{O}_{16}$ : C 12.01, H 1.01, N 3.50, S 24.04%. Found: C 15.63, H 1.08, N 4.32, S 23.81%.

### 3.4.3.7 Me-4-Tz with $\text{CuSO}_4 \cdot 5\text{H}_2\text{O}$

$\text{CuSO}_4 \cdot 5\text{H}_2\text{O}$  (0.5054 g 0.0031 mol) and Me-4-Tz (0.5146 g 0.0026 mol) were added in the same Schlenk tube. Anhydrous methanol (13 mL) was added to a flask and the contents dissolved. The mixture was heated to reflux under nitrogen gas with heating for 1h. The solution was cooled to room temperature filtered by the suction filtration to give a light blue solid was obtained from copper solution. Product analyses for  $\text{L} \cdot \text{CuSO}_4$ ; Analysis. Calcd. for  $\text{C}_8\text{H}_8\text{N}_2\text{CuO}_4\text{S}_3$ : C 27.00, H 2.27, N 7.87, S 27.03 %. Found: C 24.38, H 2.18, N 7.01, S 24.85 %.

## Chapter 4

### Ag(I) coordination compounds with bithiazole dinitriles

#### 4.1 Ag(I) coordination

Ag(I) is a  $d^{10}$  metal although it is significantly large and polarizes easily.<sup>45</sup> The latter property allows Ag(I) to be used to generate metal-organic frameworks with predictable crystal structures (crystal engineering)<sup>26-27</sup> i.e. Phosphines, pyridyls, pyrimidine etc.

##### 4.1.1 Alkyl dinitriles

Alkyl nitriles can be formed using very mild conditions.<sup>46</sup> Many examples of nitrile ligands for silver(I) have been structurally characterized, often these ligands are alkyl chains with one nitrile located at each end. These bridging nitriles link silver(I) centers to generate coordination polymers and networks.<sup>47-48</sup> In these cases, the alkyl bridge is structurally inert, and unable to coordinate to silver(I) or other metals.

##### 4.1.2 Phenyl nitriles

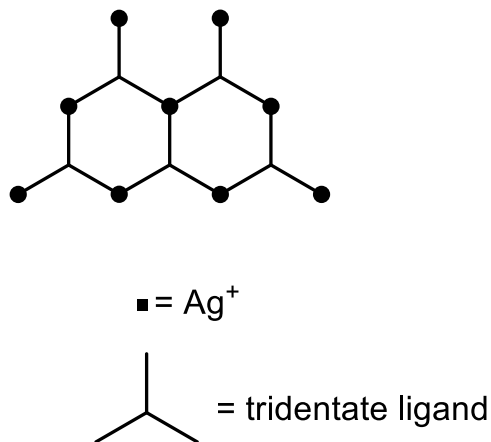
The coordination of silver ions with aryl nitriles is also common. The level of preorganization of the ligand can give rise to predictable solid-state structures. For instance, two-dimensional hexagonal networks can be made from 1,3,5-substituted benzenes,<sup>49</sup> or three-dimensional diamondoid networks when the correct shape and stoichiometry of dinitrile ligands<sup>50</sup> are used.

The coordination of nitriles with metals is also marked by changes in the spectra of the ligands, with a small but consistent increase in the stretching frequency of the nitrile

vibration, in IR absorption spectroscopy.<sup>42</sup> The stretch is diagnostic, clearly indicating coordination (or not).

#### 4.1.3 Coordination-active bridges

The alkyl and phenyl cores of the ligands discussed above are unable to coordinate to silver(I). If heteroatoms containing lone pairs are included in the bridge, the opportunity for additional links between the ligand and a metal center are possible. For example, nitrogen-containing heterocyclic rings may also bind to the  $d^{10}$  silver(I) through the ring-nitrogen, as seen in the 5,5'-dicyano-2,2'-bipyridyl ligand.<sup>51</sup> In this case, instead of simple 1-dimensional coordination polymers as found for a biphenyl bridge, a 2-dimensional network is created where the bipy core of the ligand cross-hatches the coordination polymers.



As has already been noted in this thesis, the bithiazole core has the same potential  $N, N'$ -chelating core as bipy. Therefore, research is ongoing in the MacKinnon group to generate coordination polymers using bithiazole-bridged dinitriles as ligands for silver(I).

## 4.2 General synthesis of Ag(I) dinitrile coordination complexes

Transition metals such as Ag(I) are used for reactions with organic nitrile complexes since the organonitriles show a high affinity for the silver(I) cation. In our preparations we used Ag(I) salts with complex counterions, in aromatic solvents like benzene or toluene. The mixtures were heated in sealed tubes using purified solvents. Degassing and drying of the solvents is important because under the synthetic conditions employed, silver(I) will react with oxygen or water to generate silver oxides. The sealed tubes are heated until the solids are dissolved, 90-110°C depending on the solvent, then slow-cooled at 1°C per hour to grow X-ray-quality crystals.

Several of these coordination compounds have been characterized by single-crystal X-ray diffraction. The physical properties of the resulting compounds, especially the stability of the coordination network will be investigated. This required re-synthesizing all the known compounds in sufficient quantities to perform thermogravimetric analysis (TGA), differential scanning calorimetry (DSC), and X-ray powder diffraction (XRD).

## 4.3 Results and Discussion

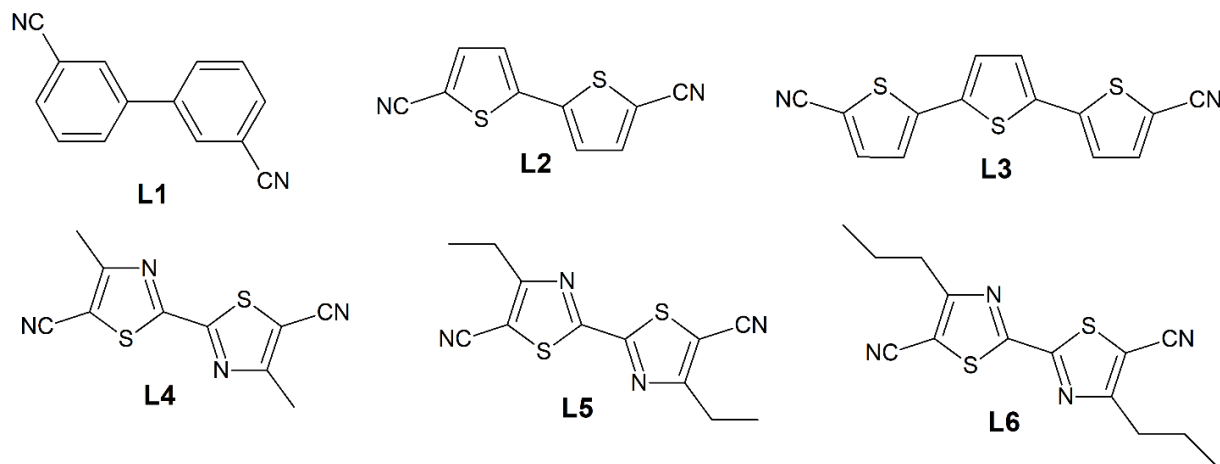


Figure 4.1: Ligands used in this study



Table 4.1: Structure of Metal–organic frameworks synthesized for this study (ratios are those observed in the single-crystal X-ray structure)

Coordination Compound	Ligand	Silver salt	Solvent	Ratio ligand: salt: solvent
12	L1	AgClO <sub>4</sub>	C <sub>6</sub> H <sub>6</sub>	1:1:1
13	L1	AgBF <sub>4</sub>	C <sub>7</sub> H <sub>8</sub>	1:1:1
14	L2	AgSO <sub>3</sub> CF <sub>3</sub>	C <sub>6</sub> H <sub>6</sub>	1:1:1
15	L3	AgBF <sub>4</sub>	C <sub>6</sub> H <sub>5</sub> NO <sub>2</sub>	1:1:1
16	L3	AgBF <sub>4</sub>	C <sub>7</sub> H <sub>8</sub>	1:1:1
17	L3	AgSO <sub>3</sub> CF <sub>3</sub>	C <sub>6</sub> H <sub>6</sub>	1:1:1
18	L4	AgClO <sub>4</sub>	C <sub>6</sub> H <sub>6</sub>	1:2:1
19	L4	AgClO <sub>4</sub>	C <sub>7</sub> H <sub>8</sub>	1:2:1
20	L5	AgBF <sub>4</sub>	C <sub>7</sub> H <sub>8</sub>	1:1:1
21	L6	AgClO <sub>4</sub>	C <sub>6</sub> H <sub>6</sub>	1:1:1
22	L6	AgBF <sub>4</sub>	C <sub>6</sub> H <sub>6</sub>	1:1:1

A large number of the silver(I)-nitrile crystal structures that have been solved – both published<sup>42,52,53</sup> and unpublished – have porous structures, where solvent molecules are incorporated into the crystal structure. In most cases these solvent molecules appear to be filling gaps, rather than acting as weakly-coordinated ligands. One such example is complex **14**, shown in **Figure 4.2**. Porous structures are interesting for potential applications in gas storage or chemical sensors, so we set out to determine the physical nature of the molecules of solvation.

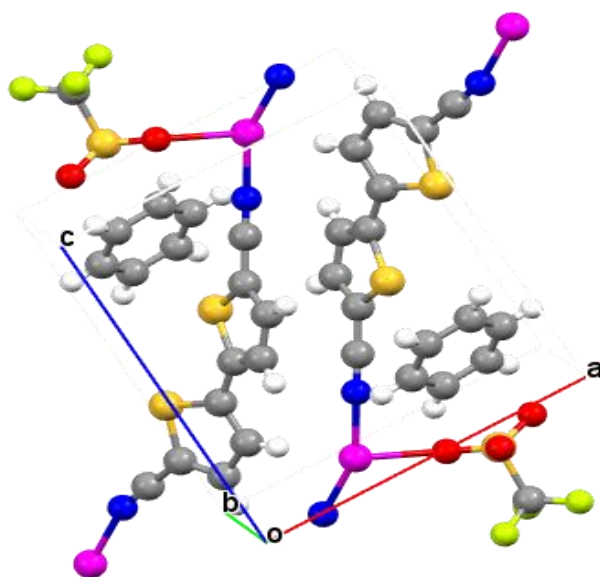


Figure 4.2: Single crystal structure unit cell of compound **14**

We first wanted to see if the solvent molecules could be easily removed, thus turning to thermogravimetric analysis (TGA). The six ligands for which we have the crystal structure of at least one silver(I) coordination complex are shown in **Figure 4.1**. Crystalline coordination complexes were prepared (i.e. fresh crystals were prepared for each coordination compound) for those compounds known to include solvent molecules in the crystal structure; the coordination structures **12** to **22** generated from these ligands are summarized in **Table 4.1**. In our case, we see a simultaneous TGA and DSC peak when solvents of crystallization are lost.

Table 4.2: TGA results

Coordination Compound	Molecular formula	Molar mass	Mass loss	Temp	Result
12	$C_{20}H_{14}N_2AgClO_4$	489.67g/mol	-7.43 %	150.1-154.5 °C	- ½ benzene
13	$C_{21}H_{16}N_2AgBF_4$	382.2g/mol	-1.49 %	178.4-193.0 °C	effectively no solvent loss
14	$C_{17}H_{10}S_3N_2AgO_3F_3$	550.2g/mol	-7.75 %	97.3-108.9 °C	- ½ benzene
15	$C_{20}H_{11}S_3N_3O_2AgBF_4$	615g/mol			decomposes without any other change
16	$C_{21}H_{14}S_3N_2AgBF_4$	584.2g/mol	-7.72 %	145.5-157.3 °C	- ½ toluene
17	$C_{21}H_{12}S_4N_2AgO_3F_3$	632.2g/mol	-8.08 %	127.3-137.3 °C	- 2/3 benzene
18	$C_{16}H_{12}S_2N_4AgClO_4$	530.4g/mol	-3.71 %	234.1-253.2 °C	- ¼ benzene
19	$C_{17}H_{14}S_2N_4AgClO_4$	544.4g/mol	-7.62 %	146.8-155.3 °C	- ½ toluene
20	$C_{19}H_{18}S_2N_4AgBF_4$	560.2g/mol	-11.95 %	109.4-116.8 °C	- 1 toluene
21	$C_{20}H_{20}S_2N_4AgClO_4$	586.4g/mol	-3.65 %	139.6-145.6 °C	- ¼ benzene
22	$C_{20}H_{20}S_2N_4AgBF_4$	574.2g/mol	-5.36 %	167.5-178.0 °C	- 1/3 benzene

To obtain the results in **Table 4.2**, we used a heating rate of five degrees per minute, up to a maximum of 250 °C. The last column of this table shows how much solvent was lost from each compound. Surprisingly, there is only one example where the entire solvent of crystallization is lost, rather, there does seem to be a remarkably consistent loss of approximately half the solvent molecules across the majority of the complexes tested. The TGA/DSC traces for all the compounds in **Table 4.2**. are shown in the figures below.

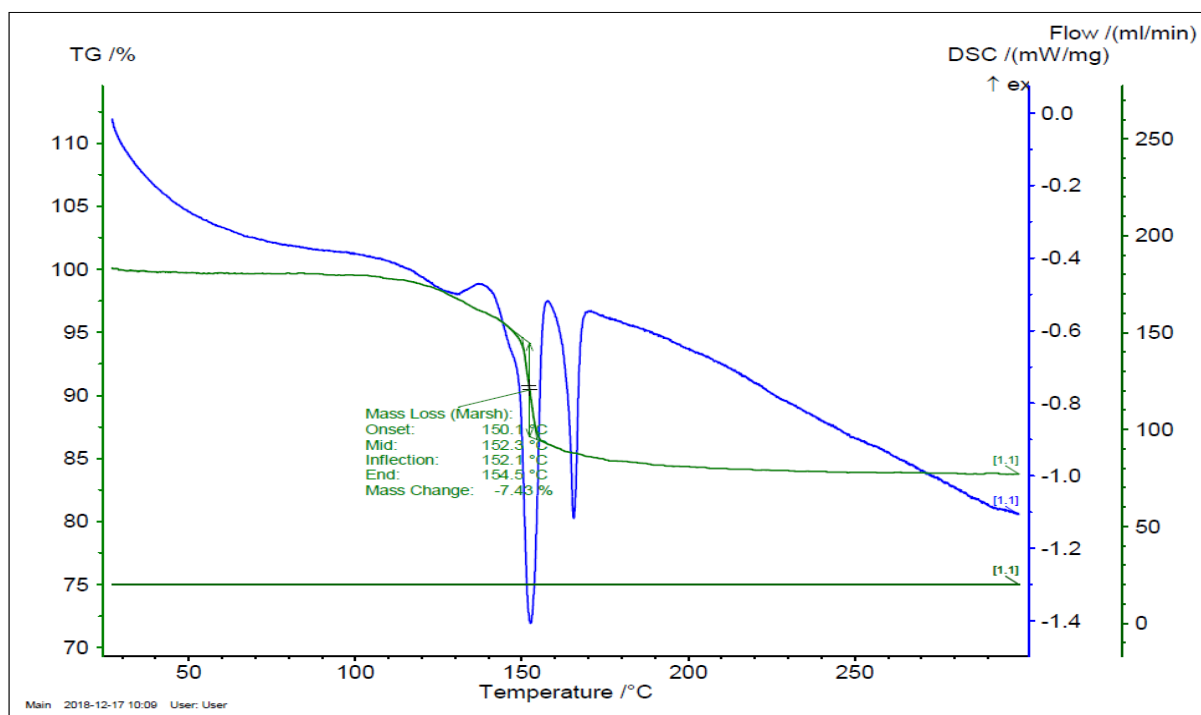


Figure 4.3: TGA and DSC for Compound 12

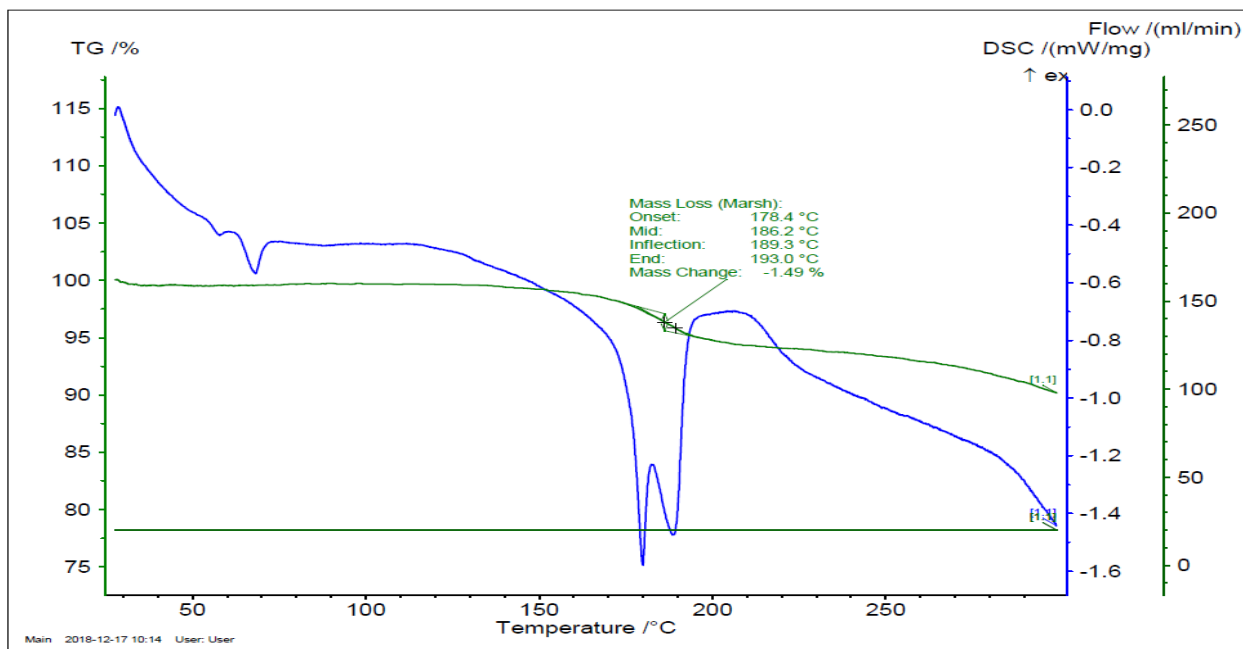


Figure 4.4: TGA and DSC for Compound 13

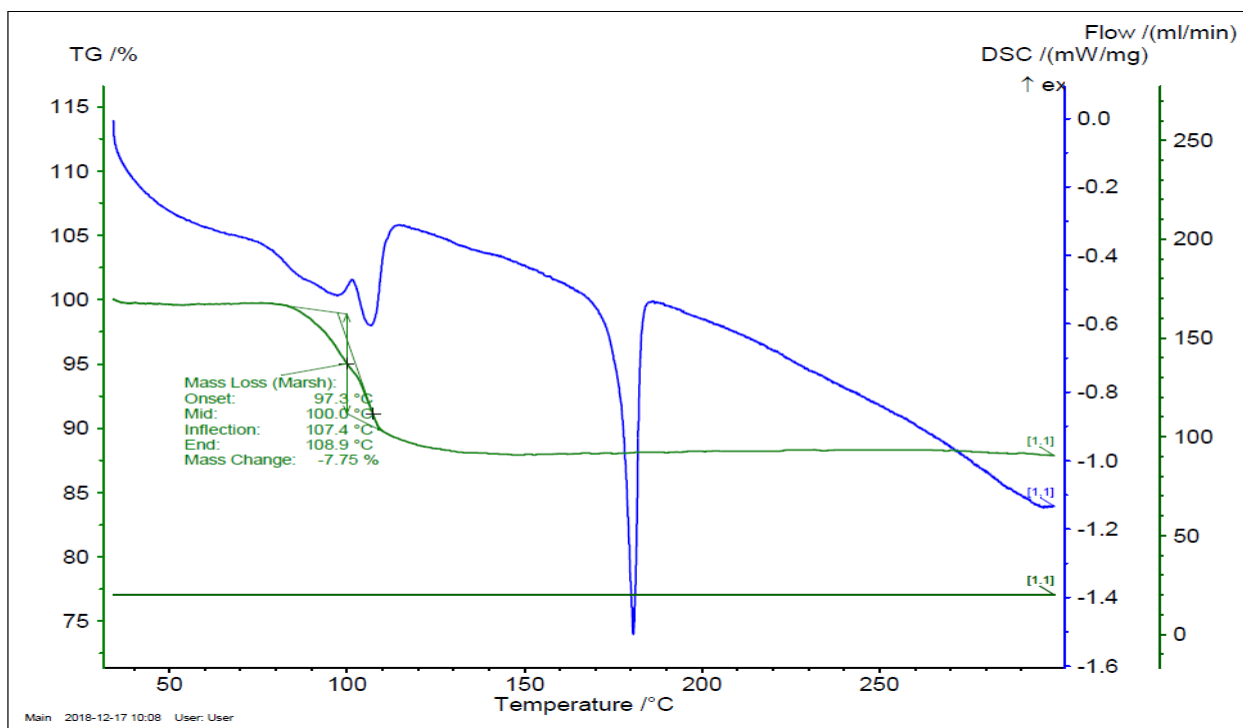


Figure 4.5: TGA and DSC for Compound 14

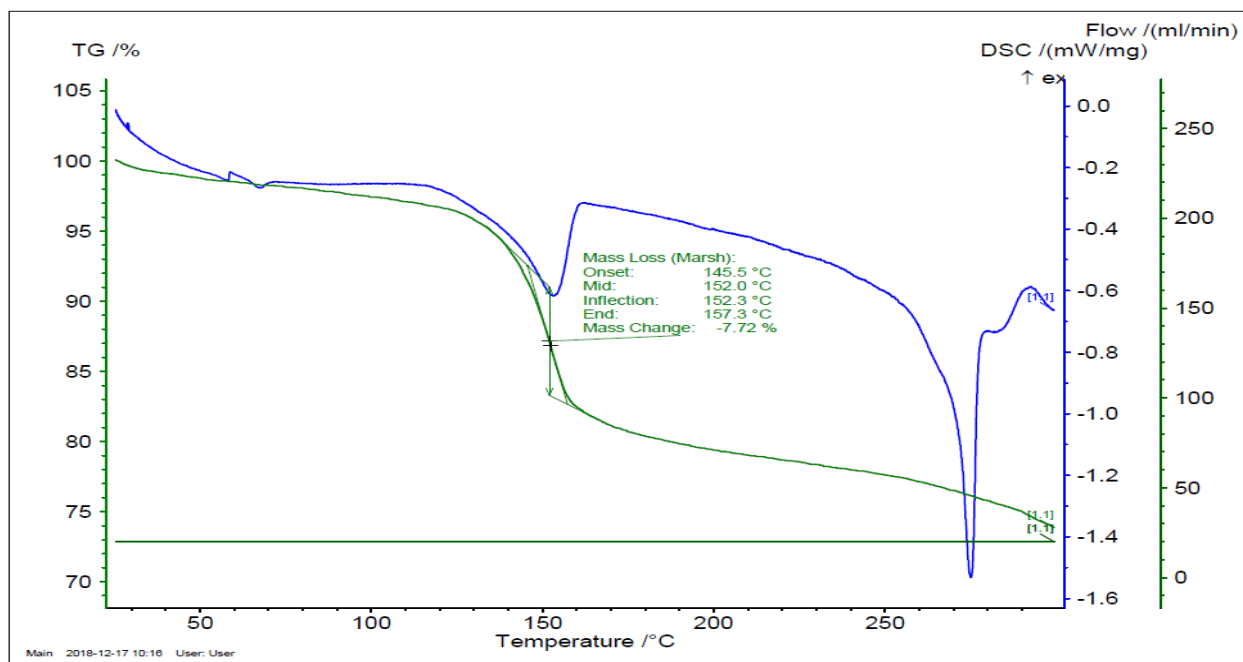


Figure 4.6: TGA and DSC for Compound 15

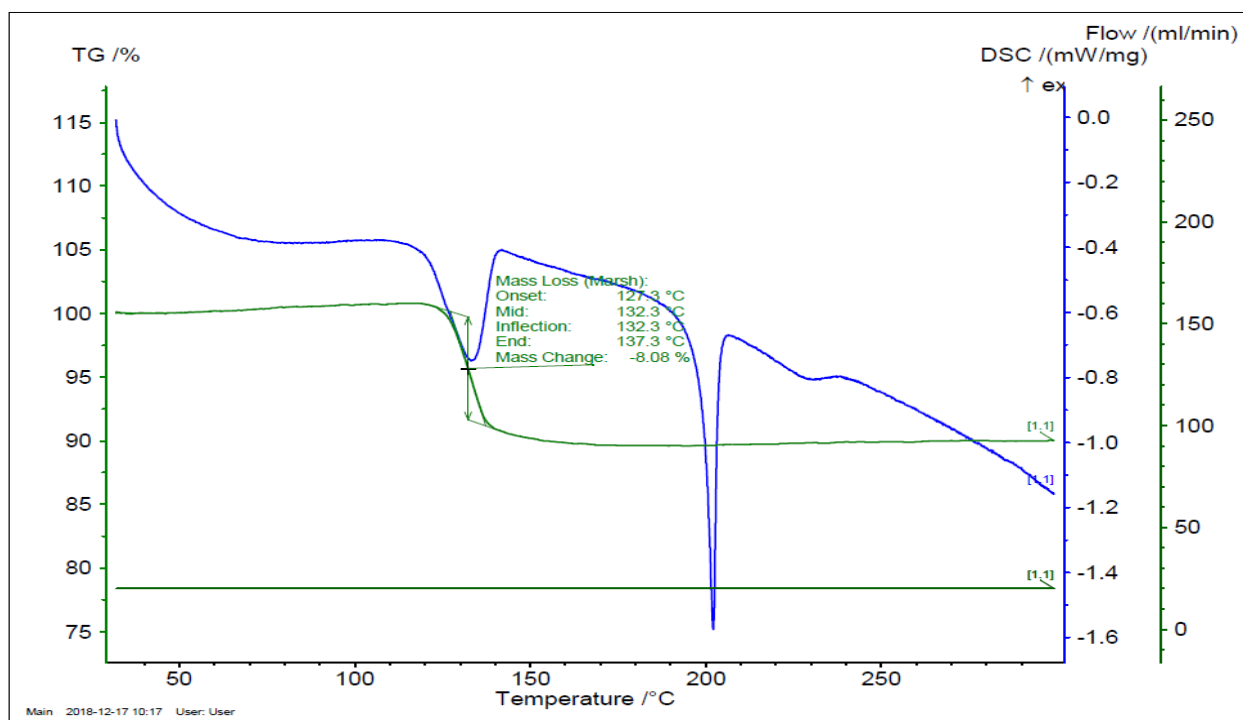


Figure 4.7: TGA and DSC for Compound 16

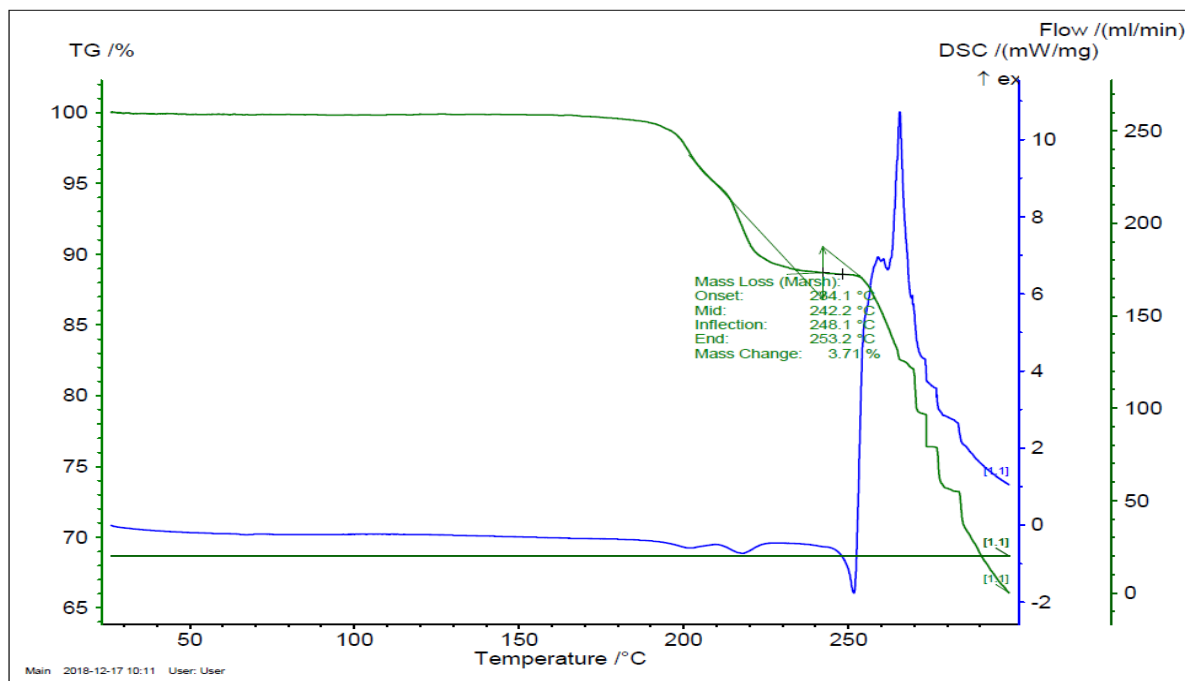


Figure 4.8: TGA and DSC for Compound 17

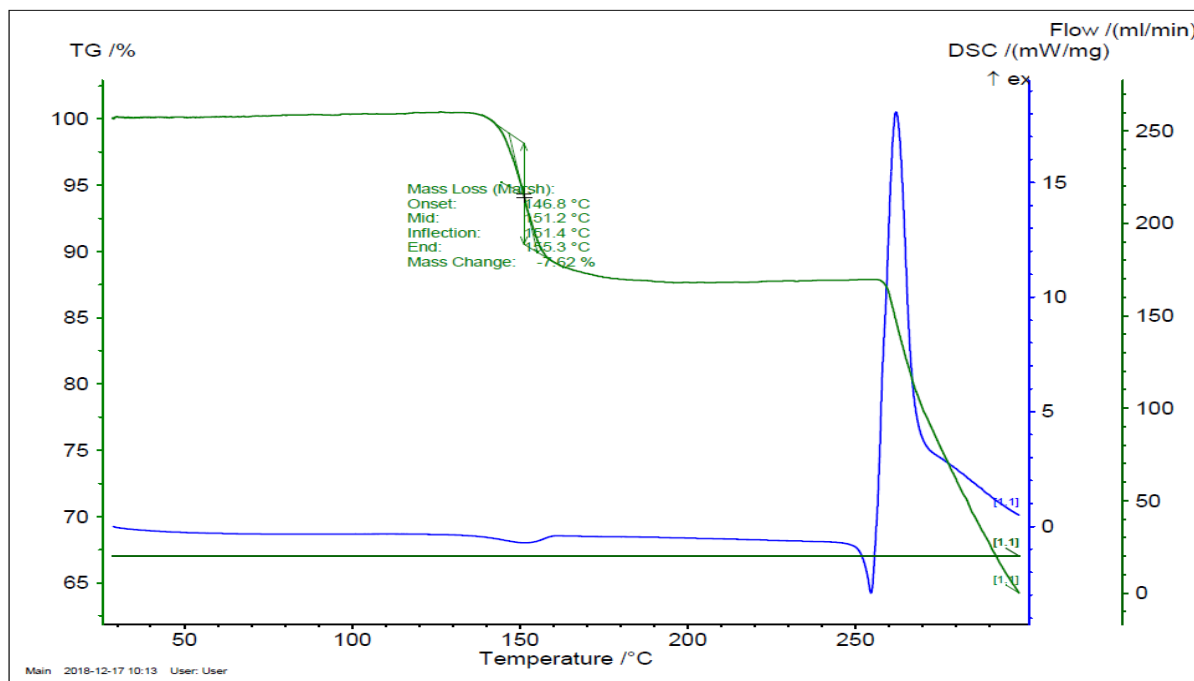


Figure 4.9: TGA and DSC for Compound 18

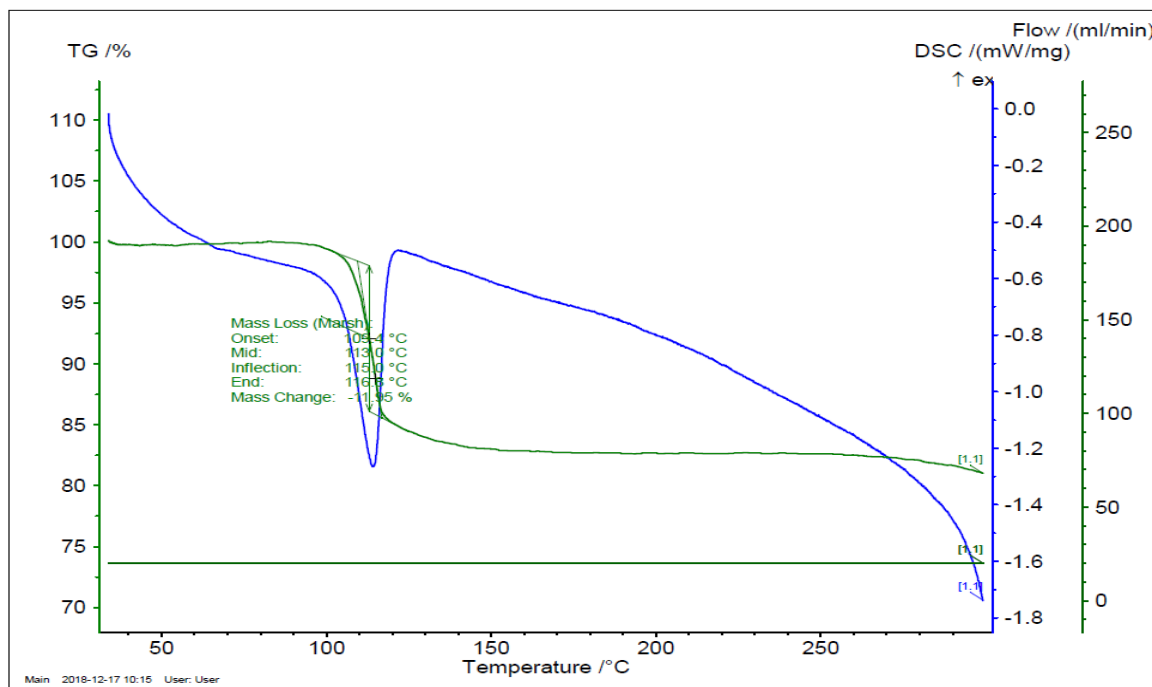


Figure 4.10: TGA and DSC for Compound 19

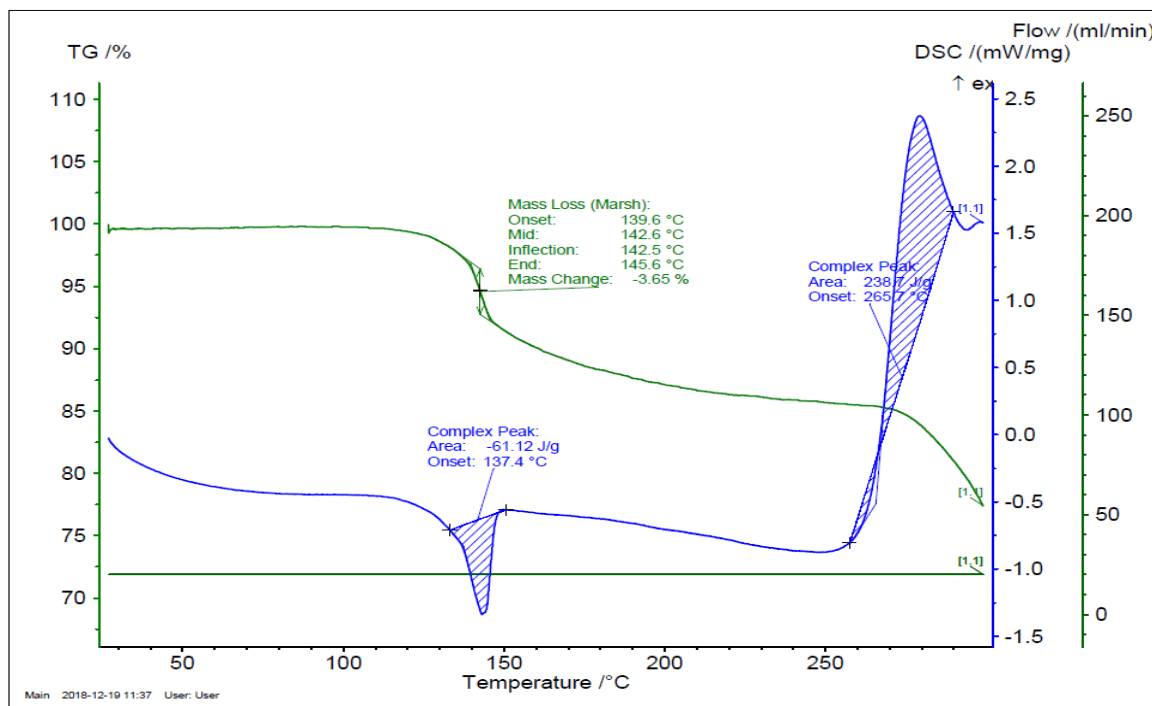


Figure 4.11: TGA and DSC for Compound 20



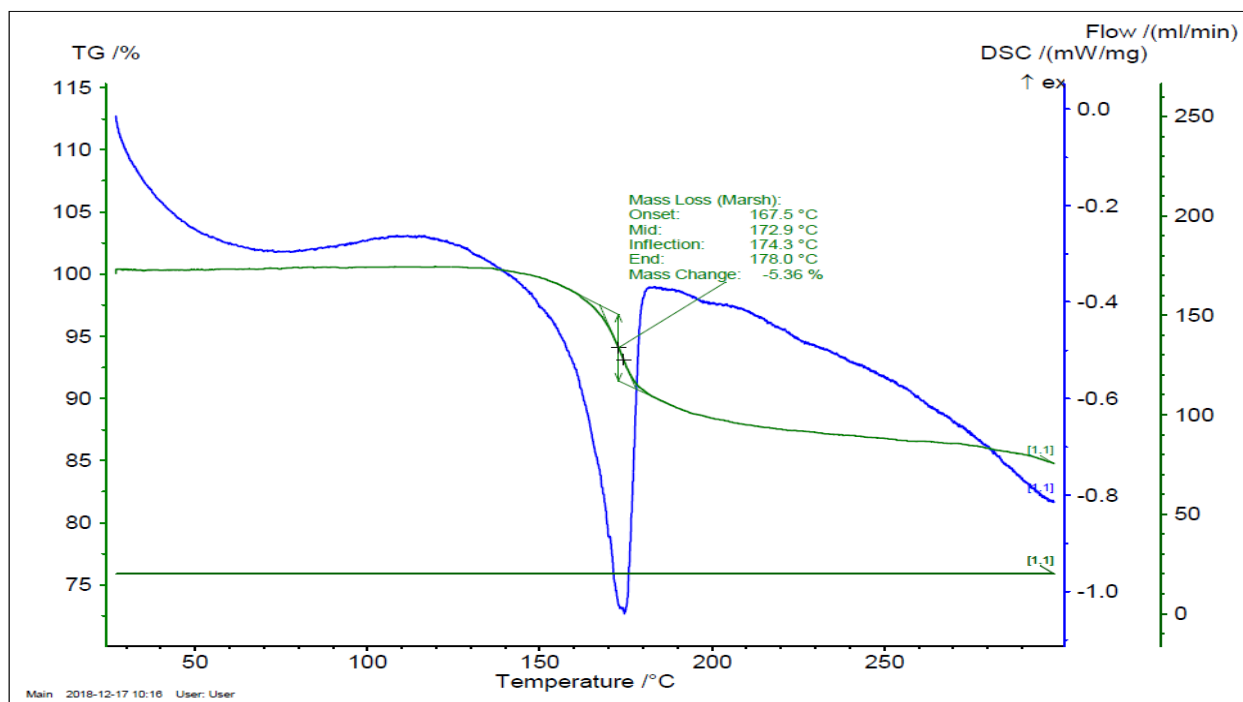


Figure 4.12: TGA and DSC for Compound **21**

#### 4.3.1 DSC analysis

In all cases, a differential scanning calorimetry (DSC) scan was run simultaneously with the TGA. In each case, there is an endothermic DSC peak coincident with the TGA mass loss, as expected. In addition, in most cases, there was a significant additional endothermic peak following the mass-loss peak, which did not have a corresponding TGA peak. We attribute this second DSC peak to a phase transition. The melting points for compound **12**(140°C -160°C), compound **14**(170°C -178°C), compound **16**(205°C - 245°C). correspond to this second endothermic peak.

Some of the melting points reported here are necessarily broad because it is difficult to visually distinguish between solvent loss and melting in a simple melting-point

apparatus (i.e. if the two transitions are close in temperature, it looks like one continuous phase change), hence the need for DSC data to distinguish what is happening. It is unclear from this data whether the solvent loss triggers a phase change to a new high-temperature phase. In these cases, could explain, why the structure stops losing solvent. Potentially the new phase holds the remaining solvent more tightly.

### 4.3.2 XRD

To determine if the MOF structures survive the loss of the solvents of crystallization, X-ray powder diffraction was performed on “desolvated” material. Crystalline material of each complex was heated to the mass-loss temperature (as given in Table 4.3) under vacuum to simulate the TGA conditions. Powder XRD was then performed on the resulting material. We also used XRD to examine our materials after they have been heated to determine if there is any change in the crystalline structure other than the removal of the (usually disordered) solvent molecules.

Table 4.3: XRD result for all complexes after heating

Compound	Ligand	Silver salt	Solvent	Structure	XRD after heating
12	<i>m</i> -Ph <sub>2</sub> CN <sub>2</sub>	AgClO <sub>4</sub>	C <sub>6</sub> H <sub>6</sub>	1:1:1	Significant overlap between simulated and actual
14	T <sub>2</sub> CN <sub>2</sub>	AgSO <sub>3</sub> CF <sub>3</sub>	C <sub>6</sub> H <sub>6</sub>	1:1:1	loss of crystallinity
15	T <sub>3</sub> CN <sub>2</sub>	AgBF <sub>4</sub>	C <sub>6</sub> H <sub>5</sub> NO <sub>2</sub>	1:1:1	Decomposition during TGA
16	T <sub>3</sub> CN <sub>2</sub>	AgBF <sub>4</sub>	C <sub>7</sub> H <sub>8</sub>	1:1:1	one line in measured XRD, which doesn't line up with sim
17	T <sub>3</sub> CN <sub>2</sub>	AgSO <sub>3</sub> CF <sub>3</sub>	C <sub>6</sub> H <sub>6</sub>	1:1:1	loss of crystallinity
18	MeTz <sub>2</sub> CN <sub>2</sub>	AgClO <sub>4</sub>	C <sub>6</sub> H <sub>6</sub>	1:2:1	Significant overlap between simulated and actual

<b>19</b>	MeTz <sub>2</sub> CN <sub>2</sub>	AgClO <sub>4</sub>	C <sub>7</sub> H <sub>8</sub>	1:2:1	crystalline, but little overlap with simulated spectrum
<b>20</b>	EtTz <sub>2</sub> CN <sub>2</sub>	AgBF <sub>4</sub>	C <sub>7</sub> H <sub>8</sub>	1:1:1	crystalline, but little overlap with simulated spectrum
<b>21</b>	PrTz <sub>2</sub> CN <sub>2</sub>	AgClO <sub>4</sub>	C <sub>6</sub> H <sub>6</sub>	1:1:1	crystalline, but little overlap with simulated spectrum
<b>22</b>	PrTz <sub>2</sub> CN <sub>2</sub>	AgBF <sub>4</sub>	C <sub>6</sub> H <sub>6</sub>	1:1:1	crystalline, but little overlap with simulated spectrum

Two structures (**14** and **17**) have no diffraction pattern, suggesting total loss of crystallinity. Two structures (**12** and **18**) have significant overlapping peaks between the post-thermally-treated powder spectrum and the powder spectrum simulated from the single-crystal structure. This indicates a strong correlation between the unit cell parameters and the atomic positions between the structures and the retention of the underlying MOF structure throughout the heating process.

On the other hand, the remaining compounds have strong powder diffraction peaks in the post-heat-treated samples, indicating a crystalline material, but few peaks correspond to the simulated spectrum of the original single-crystal structure. There are two obvious potential explanations: either the single-crystal structure did not represent the bulk structure (which the XRD powder is now showing) or the structure recrystallizes into a new form following loss of solvent (the underlying MOF is not strong enough to support the vacancies and undergoes a phase transition). We believe the latter to be the case, because we have additional evidence (e.g. multiple single crystals indexed, consistent combustion analysis) that suggests that the single crystals are in fact representative of the bulk.

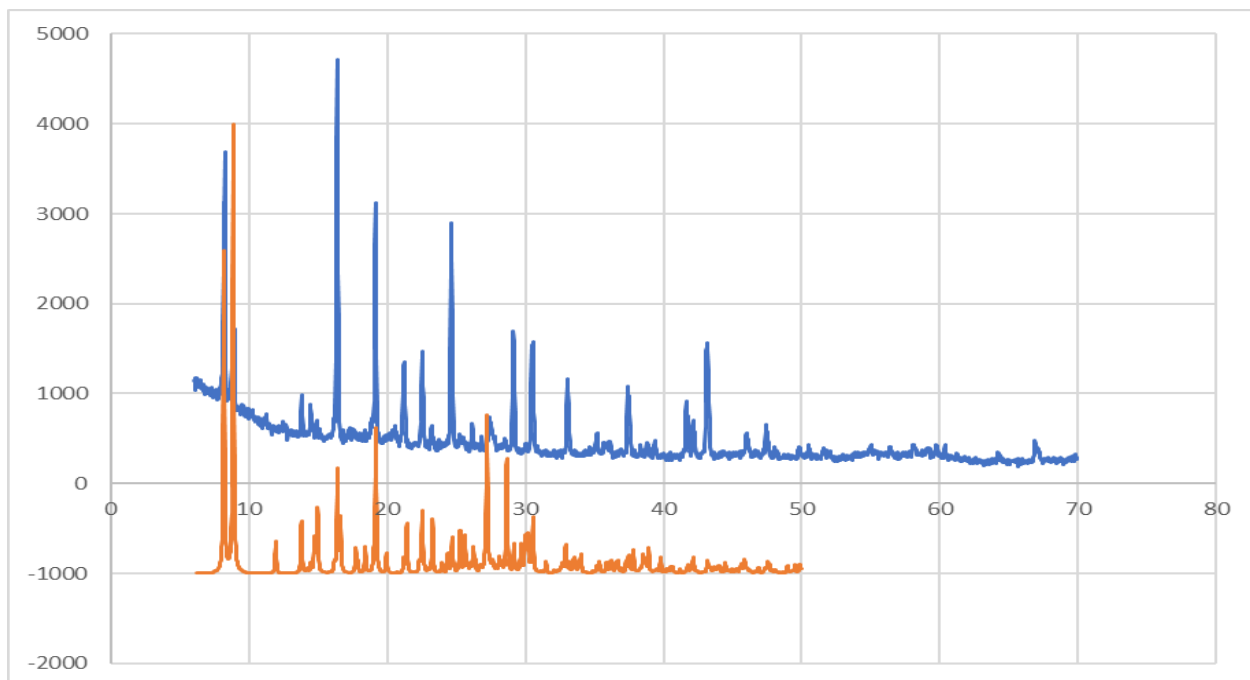


Figure 4.13: Experimental (blue) and simulated(orange) XRD spectra of Compound **12**

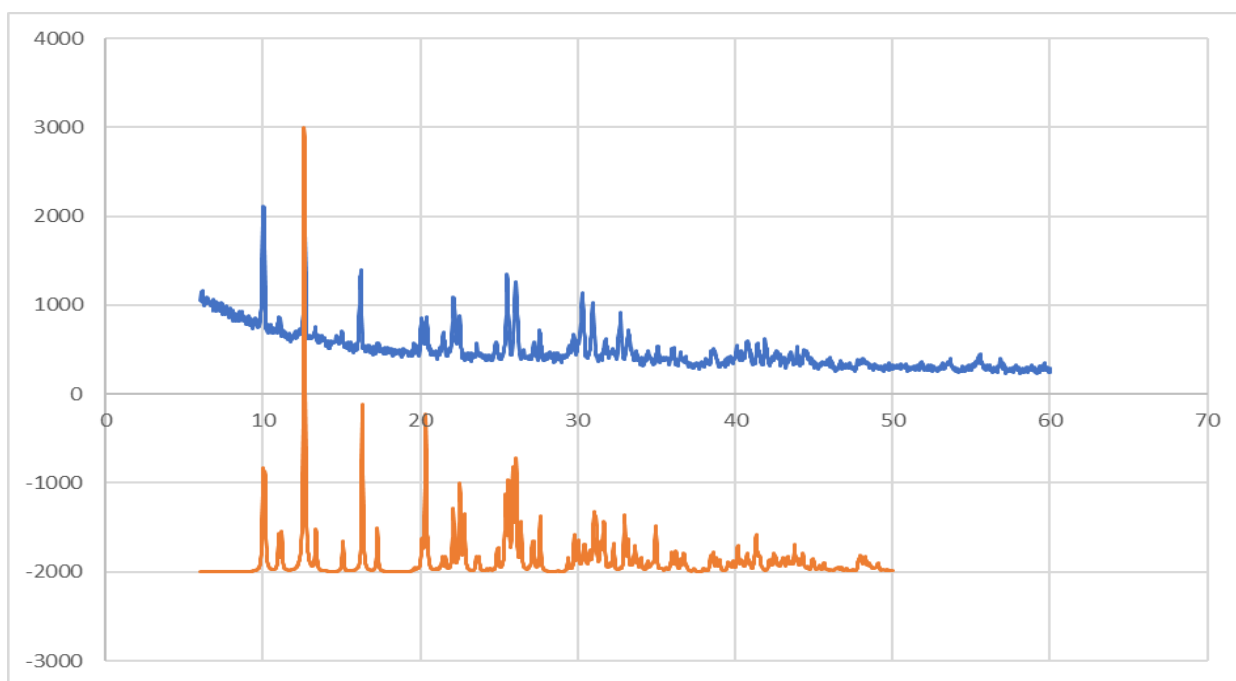


Figure 4.14: Experimental (blue) and simulated(orange) XRD spectra of Compound **18**

## 4.4 Conclusion

The reactions between various aromatic dinitriles and silver(I) salts were carried out in various solvents and with various metal: ligand ratios, yielding several new coordination complexes. Crystalline materials were isolated for these coordination complexes. The resulting products for several reactions were confirmed to be coordination complexes. After heating the structure is not preserved except in two cases, compounds **12** and **18**. The TGA/DSC analyses for all the compounds have been done to show how much solvent was lost from each compound. In most cases, around 50% of the solvent was lost during TGA. It can be concluded that the solvents serve a significant purpose in most of the crystal structures, in maintaining the MOF structure, even though the solvents are not coordinating to the metal. In most cases, loss of these supports causes a phase change or loss of crystallinity. However, in two cases, **12** and **18**, there appears to be consistency between the original crystal structure and the solid-state structure post-solvent-loss, suggesting these MOFs are more robust than the rest.

## 4.5 Experimental

### 4.5.1 Instrumental techniques used

Thermogravimetric Analysis (TGA) measures the amount of weight change of a material, either as a function of increasing temperature, or isothermally as a function of time, in an atmosphere of nitrogen, helium, air, other gas, or in vacuum.

Differential scanning calorimetry (DSC) can be run simultaneously with TGA. Instead of heat loss, it measures temperature change of a sample compared to an inert substance. If the sample undergoes an endothermic phase change (e.g. melting), rate of

temperature change in the sample will stop while the heat is used to perform the phase change.

X-ray Powder Diffraction (XRD) is used for phase identification of a crystalline material and can provide information on unit cell dimensions. The sample rotates in the path of a collimated X-ray beam at an angle  $\theta$  while the detector collects the diffracted X-rays. The device used to maintain the angle and rotate the sample is termed a goniometer.

TGA and DSC measurements were taken on a Netzsch STA 449 F3 Jupiter with parameters set to heat from 30 °C to 300 °C at 5 °C/min and hold at 300 °C for 5 min. XRD was measured on PANalytical with diffractometer system X'Pert-PRO parameters start position [ $^{\circ}2\theta$ ] 6.0331 and end position [ $^{\circ}2\theta$ ] 96.9291, scan step time [s] 37.7400 at measurement temperature 25 °C and anode material Cu. Crystals were grown in an Applied test system, INC 3210, 3-zone tube furnace attached to an 800 °C maximum temperature-control system.

#### **4.5.2 Synthesis – general procedures and materials**

Silver salts were purchased from commercial sources and used as received. Solvents were purified by passage through an alumina column in a home-built solvent-purification system.<sup>56</sup> Compounds **12** to **17** were synthesized according to the published procedures.<sup>53-55</sup> Ligands **L4** to **L6** were synthesized by adaptation of the literature procedure, changing the ketone to give the correct alkyl chain length.<sup>57</sup>

#### **4.5.3 Synthesis of coordination compounds**

*General Procedure.* Ligand and metal salt were added to a homemade Pyrex reaction tube 20 mm OD by 25 cm long. Purified solvent was added, and the contents frozen to

allow the tube to be sealed under vacuum. The contents were placed in a tube furnace and heated to an initial temperature, stabilized for two hours, then cooled at a rate of 1°C per hour until room temperature was reached.

*Synthesis of compound 18.* Silver(I) perchlorate (30.0 mg, 144.7  $\mu\text{mol}$ ) and ligand **L4** (17.0 mg, 52.46  $\mu\text{mol}$ ) with benzene as solvent was heated to 90°C.

*Synthesis of compound 19.* Silver(I) perchlorate (30.0 mg, 144.7  $\mu\text{mol}$ ) and ligand **L4** (18.0 mg, 53.25  $\mu\text{mol}$ ) with toluene as solvent was heated to 110°C.

*Synthesis of compound 20.* Silver(I) tetrafluoroborate (15.5 mg, 79.62  $\mu\text{mol}$ ) and ligand **L5** (20.2 mg, 55.19  $\mu\text{mol}$ ) with toluene as solvent was heated to 110°C.

*Synthesis of compound 21.* Silver(I) perchlorate (18.0 mg, 86.82  $\mu\text{mol}$ ) and ligand **L6** (25.0 mg, 65.78  $\mu\text{mol}$ ) with benzene as solvent was heated to 90°C.

*Synthesis of compound 22.* Silver(I) tetrafluoroborate (26.3 mg, 135.1  $\mu\text{mol}$ ) and ligand **L6** (20.3 mg, 53.42  $\mu\text{mol}$ ) with benzene as solvent was heated to 90°C.

## Chapter 5

### General Conclusions and Future Direction

#### 5.1 Conclusion

In this thesis, the syntheses of new bithiazoles are presented for 2,2'-dichloro-4,4'-bithiazole, 5,5'-dibromo-2,2'-dimethyl-4,4'-bithiazole, and 5,5'-dibromo-2,2'-diamino-4,4'-bithiazole. The synthesis of new dinitrile ligands have also been accomplished. IR spectroscopy shows the conversion of a chlorobithiazole and an aminobithiazole to dinitriles. Unfortunately, a method of reliably purifying these new ligands has not yet been found, therefore it was not possible to isolate any new silver(I)-dinitrile MOFs.

Purification has been a difficulty, perhaps due to the basic nature of the thiazole ring nitrogens. Unfortunately, the need to maintain basic conditions to avoid protonating the ring nitrogens may render these synthetic routes untenable, since organic nitriles are easily hydrolyzed under basic conditions. Luckily, there are many routes to aromatic nitriles, another may be discovered to be better than the routes presented here, and which will be investigated in the future in the MacKinnon lab e.g. dehydration of an amide with  $\text{SOCl}_2$  or the Letts synthesis.

The first systematic comparison of the coordination chemistry of 5,5'-dimethyl-2,2'-bipyridyl (Me-bipy), and 2,2'-dimethyl-4,4'-bithiazole (Me-4Tz) with various metal cations has been accomplished. Reactions were screened using UV-visible absorption spectroscopy. It appears that bithiazole ligands do not bind as strongly as bipy ligands as indicated by the lack of shift in the UV-visible ligand spectrum as observed in the bithiazole cases. This is in marked contrast to dilute solutions containing the same metal



salts with dimethyl-bipy, which show significant ligand shifts in the  $\lambda_{\text{MAX}}$  for cations  $\text{Al}^{3+}$ ,  $\text{Cr}^{3+}$ ,  $\text{Ni}^{2+}$ ,  $\text{Y}^{3+}$ ,  $\text{Cd}^{2+}$ , and,  $\text{Pb}^{2+}$ . Due to the fact that the bithiazole compounds do not show a strong affinity for binding to heavy metals, it was confirmed that bipyridyl compounds are more effective at binding heavy metals than bithiazole compounds.

Larger-scale reactions were performed using 2,2'-dimethyl-4,4'-bithiazole as a ligand. We used cations that have been shown to form coordination compounds with bithiazole ligands. A solid was isolated, and observation of a colour change from the starting material, suggest a change in the coordination sphere of the metal. The solids were also characterized by combustion analysis.

One bithiazole MOF system that has been well characterized is that of substituted 2,2'-bithiophene dinitriles with silver(I). Several crystal structures have been solved, as well as silver(I)-nitrile systems with oligophenyl-dinitriles and oligothiophene-dinitriles. In order to characterize the thermal stability of these systems, TGA, DSC, and X-ray powder diffraction data were collected on freshly-prepared crystalline samples. A common theme in these structures is that they tend to trap solvent molecules in the MOF structure. The TGA data suggests that these solvent molecules can be removed, but on average only about half of a solvent molecule per ligand. The XRD data taken after loss of solvent suggests that most complexes do not retain their original crystal structure prior to heating, with the exception of compounds **12** and **18**, which appear to maintain their structures.

## **5.2 Future directions**

### **5.2.1 Direct continued work**

The work presented in this thesis suggests a number of possible additional experiments that, due to time constraints, could not be carried out. These experiments could easily be expanded into future projects. First, more varieties of the bithiazole compounds could be synthesized. In fact, one of the general goals of research in the MacKinnon group is to develop synthetic methods for generating new bithiazoles. Finding a method of purifying the dicyano-4,4'-bithiazole, or a better synthetic route, remains a primary goal, so that a direct comparison of the binding abilities of 2,2' and 4,4' bithiazoles with the silver(I) cation can be performed. Further characterization of the various methyl and amino bithiazoles with other metal cations will be pursued, with the object of solving crystal structures of 2,2'-derivatives to compare with the 4,4'-derivatives known from the literature.

### **5.2.2 Potential future projects**

The bithiazole system has many potential uses, but synthetic methodology needs to be developed to unlock the potential of this ligand system, which is an ongoing focus of the Mackinnon research program. Uses for this ligand system would range from pharmaceuticals to energy conversion to chemical sensors, but each use will require the development of synthetic method for functionalization and/or coordination chemistry of the bithiazole core system.

Radiopharmaceuticals are examples of radiocompounds that can be used as therapeutic agents to diagnosis a particular condition. The application of these

pharmaceutical drugs will continue to grow because clinical scientists will use them alongside imaging devices to deliver appropriate treatments in the future. Overall, scientists are using radiopharmaceuticals as diagnostic agents to treat various diseases. Drugs containing bithiazoles are already used in various treatments. Finding methods of coordinating these bithiazole units with radioisotopes would allow diagnostic investigations of the mechanisms of these drugs.

Bithiazole has also acquired importance due to its inclusion into semiconductors and its ability to improve the effectiveness of solar cells. The bithiazole has resulted in an improved activity when inserted into solar cells<sup>19</sup>.

Chemical sensors are compounds that act as analyzers and transform biochemical information into useful signals analytically. Bithiazoles could be incorporated into such sensors since the binding centers of the ring nitrogen's are parts of conjugated rings. As such any change in the conjugation, *e.g.* electron donation to a metal center, could result in a colour, photoemission, or other measurable electronic change. Thus, much potential exists regarding the effectiveness and utility of bithiazole compounds.

## Chapter 6

### References

1. Crabtree, R. H. The organometallic chemistry of the transition metals, 3rd.; John Wiley & Sons: New York, NY, **2001**.
2. Zhou, H.; Long, R. J.; Yaghi, M. O. *Chem. Rev.* **2012**, *112*, 673.
3. Atkins, P. W.; Overton, T. L.; Rourke, J. P.; Weller, M. T.; Armstrong, F. A. Shriver & Atkins' Inorganic Chemistry, 5th.; Oxford University Press, New York, NY, **2010**.
4. Dzhardimalieva, I. G.; Uflyand, E. I. *RSC. Adv.* **2017**, *7*, 42242.
5. Dogan, J.; Schulte, B. J.; Swiegers, F. G.; Wild, B. S. *J. Org. Chem.* **2000**, *65*, 951.
6. Abo-Bakr, M. A.; Hassan, A. M.; Temirek, H. H.; Mosallam, M. A. *Orient. J. Chem.* **2012**, *28*, 1567.
7. Hamzah, S. A.; Shaameri, Z.; Goksu, S. *J. Chem.* **2013**, *2013*, 1.
8. Kaes, C.; Katz, A.; Hosseini, M. W. *Chem. Rev.* **2000**, *100*, 3553.
9. Mudasir.; Yoshioka, N.; Inoue, H. *J. Coord. Chem.* **2001**, *52*, 333.
10. Helal, C. J.; Sanner, M. A.; Cooper, C. B.; Gant, T.; Adam, M.; Lucas, J. C.; Kang, Z. Kupchinsky, S.; Ahlijanian, M. K.; Tate, B.; Menniti, F. S.; Kelly, K.; Peterson, M. *Bioorg. Med. Chem. Lett.* **2004**, *14*, 5521.
11. Ghaemmaghami, S.; May, B. C. H.; Reslow, A. R.; Prusiner, S. B. *J. Virol.* **2010**, *84*, 3408.

12. Almaliti, J.; Al-Hamashi, A. A.; Negmeldin, A. T.; Hanigan, C. L.; Perera, L.; Pflum, M. K. H.; Casero, R. A. J.; Tillekeratne, L. M. V. *J. Med. Chem.* **2016**, *59*, 10642.
13. Al-Hashemi, R.; Safari, N.; Abedi, A.; Notash, B.; Amani, V.; Khavasi, R. H. *J. Coord. Chem.* **2009**, *62*, 2909.
14. Notash, B.; Amani, V.; Safari, N.; Ostad, N, S.; Abedi, A.; Dehnavi, Z, M. *Dalton Trans.* **2013**, *42*, 6852.
15. Povirk, F, L.; Hogan, M.; Dattagupta, N. *Biochemistry.* **1979**, *18*, 96.
16. Nieweg, O. E.; Beekhuis, H.; Paans, A. M. J.; Piers, D. A.; Vaalburg, W.; Welleweerd, J.; Wiegman, T.; Woldring, M. G. *Eur. J. Nucl. Med.* **1982**, *7*, 104.
17. Thomas, C.J.; McCormick, M.M.; Vialas, C.; Tao, Z.-F.; Leitheiser, C.J.; Rishel, M.J.; Wu, X.; and Hecht, S.M. *J. Am. Chem. Soc.* **2002**, *124*, 3875.
18. Lighvan, M, Z.; Abedi, A.; Bordbar, M. *Poly.* **2012**, *46*, 149.
19. Su, H.; Sredojevic, N, D.; Bronstein, H.; Marks, J, T.; Schroeder, C, B.; Al-Hashimi, M. *Macromol. Rapid Commun.* **2017**,*38*, 1600610.
20. Zhang, M.; Fan, H.; Guo, X.; He, Y.; Zhang, Z.; Min, J.; Zhang, J.; Zhao, G.; Zhan, X.; Li, Y. *Macromolecules.* **2010**, *43*, 5706.
21. Hu, B.; Tao, T.; Bin, Z.-Y.; Peng, Y.-X.; Ma, B.-B.; Huang, W. *Cryst. Growth Des.* **2014**, *14*, 300.
22. Zaworotko, M. *J. Chem. Soc. Rev.* **1994**, 283.
23. Goesten, M. G.; Kapteijn, F.; Gascon, J. *CrystEngComm* **2013**, *15*, 9249.

24. Yuan, S.; Feng, L.; Wang, K.; Pang, J.; Bosch, M.; Lollar, C.; Sun, Y.; Qin, J.; Yang, X.; Zhang, P.; Wang, Q.; Zou, L.; Zhang, Y.; Zhang, L.; Fang, Y.; Li, J.; Zhou, H. *Adv. Mater.* **2018**, *30*, 1870277.
25. Njogu, M, E.; Omondi, B.; Nyamori, V. *J. Coord. Chem.* **2015**, *68*, 3389.
26. Khlobystov, A. N.; Blake, A. J.; Champness, N. R.; Lemonovskii, D. A.; Majouga, A. G.; Zyk, N. V.; Schröder, M. *Coord. Chem. Rev.* **2001**, *222*, 155.
27. Chen, C.-L.; Kang, B.-S.; Su, C.-Y. *Aust. J. Chem.* **2006**, *59*, 3.
28. Cârçu, V.; Negoiu, M.; Rosu, T.; Stoicescu, L.; Georgescu, R. *Synt. React. Inor. Meta. Orga. Chem.* **2000**, *30*, 1653.
29. Khavasi, R, H.; Abedi, A.; Amani, V.; Notash, B.; Safari, N. *Poly.* **2008**, *27*, 1848.
30. Shahbazi-Raz, F.; Notash, B.; Amani, V.; Safari, N. *Poly.* **2016**, *119*, 227.
31. Maclean, J, B.; Pickup, G, P. *J. Mate. Chem.* **2001**, *11*, 1357.
32. Hantzsch, A.; Weber, H, J. *Beri. Deut. Chem. Gese.* **1887**, *20*, 3118.
33. Ayati, A.; Emami, S.; Asadipour, A.; Shafiee, A.; Foroumadi, A. *Chem.* **2015**, *46*.
34. Yang, C.; Cui, Y. *Synth. Comm.* **2001**, *31*, 1221.
35. Notash, B.; Safari, N.; Khavasi, R, H.; Amani, V.; Abedi, A. *J. Organomet. Chem.* **2008**, *693*, 3553.
36. Lin, W.; Sun, W.; Yang, J.; Shen, Z. *Mate. Chem. Phys.* **2008**, *112*, 617.
37. Karrer, P.; Leiser, P.; Graf, W. *Helv. Chim. Acta.* **1944**, *27*, 624.

38. Paulmier, C.; Morel, J.; Pastour, P.; Semard, D. *Bull. Soc. Chim. Fr.* **1969**, 2511.
39. Armarego, W, L, F.; Perrin, D, D. *Purification of Laboratory Chemicals*. 4<sup>th</sup>. Linacre House, Jordan Hill, Oxford. Australian National University, Canberra. **1996**
40. Morsali, A.; Payheghader, M.; Poorheravi, R, M.; Jamali, F. *Z. Anorg. Allg. Chem.* **2003**, 629, 1627.
41. Shimizu, D, K.; Rebek, J. *Proc. Nat. Acad. Sci.* **1996**, 93, 4257.
42. Sears, A, W.; Hudolin, L, M.; Jenkins, A, H.; Mawhinney, C, R.; Mackinnon, D, C. *J. Coord. Chem.* **2008**, 61, 825.
43. Hosseinian, A.; Jabbari, S.; Mahjoub, R, A.; Movahedi, M. *J. Coord. Chem.* **2012**, 65, 2623.
44. Hosseinian, A.; Mahjoub, R, A. *J. Coord. Chem.* **2010**, 63, 4245.
45. Shoeib, T.; Aribi, E, H.; Siu, W, K.; Hopkinson, C, A. *J. Phys. Chem.* **2001**, 105, 710.
46. Xia, A.; Xie, X.; Chen, H.; Zhao, J.; Zhang, C.; Liu, Y. *Org. Lett.* **2018**, 20, 7735.
47. Cunha-Silva, L.; Hardie, M. *J. CrystEngComm* **2012**, 14, 3367.
48. Genuis, E. D.; Kelly, J. A.; Patel, M.; McDonald, R.; Ferguson, M. J.; Greidanus-Strom, G. *Inorg. Chem.* **2008**, 47, 6184.
49. Kiang, Y.-H.; Gardner, G. B.; Lee, S.; Xu, Z.; Lobkovsky, E. B. *J. Am. Chem. Soc.* **1999**, 121, 8204.
50. Hirsch, K. A.; Venkataraman, D.; Wilson, S. R.; Moore, J. S.; Lee, S. *J. Chem. Soc. Chem. Commun.* **1995**, 2199.

51. Wu, H.-P.; Janiak, C.; Rheinwald, G.; Lang, H. *J. Chem. Soc. Dalton Trans.* **1999**, 183.
52. Andreychuk, R, N.; Allard, R, S.; Parent, L. M, S.; Assoud, A.; Mackinnon, D, C. *Cryst. Growth Des.* **2015**, *15*, 4377.
53. MacKinnon, C. D.; Parent, S. L. M.; Mawhinney, R. C.; Assoud, A.; Robertson, C. M. *CrystEngComm* **2009**, *11*, 160.
54. Morgan, S. I.; Daleo, N, D.; Hudolin, L, M.; Chen, A.; Assoud, A.; Jenkins, A, H.; Mackinnon, D, C. *J. Mater. Chem.* **2009**, *19*, 8162.
55. Sears, W. M.; Mackinnon, D, C.; Kraft, M, T. *Synth. Meta.* **2011**, *161*, 1655.
56. Pangborn, A. B.; Giardello, M. A.; Grubbs, R. H.; Rosen, R. K.; Timmers, F. J. *Organometallics* **1996**, *15*, 1518.
57. Nanos, J. I.; Kampf, J. W.; Curtis, M. D. *Chem. Mater.* **1995**, *7*, 2232



## Appendix

### Appendix 1: Literature syntheses as performed for this thesis

#### A1.1 Preparation of 2,2'-dimethyl-4,4'-bithiazole<sup>14,35</sup>

To a two-necked round-bottom flask equipped with a stir bar and reflux condenser was added 1,4-dibromo-2,3-butanedione (4.00g, 16.40mmol), and thioacetamide (2.49g, 33.14mmol) in the same flask and filled with nitrogen gas under heating 65°C. To this, dry degassed methanol (50ml) was added. The mixture was allowed to reflux for approximately 3 hours. Once cooled, 50 ml of distilled water was added to the mixture, which was then neutralized using 5% Na<sub>2</sub>CO<sub>3</sub> until the pH becomes approximately 9. The solution was suction filtered and then left to dry. The following obtained was light brown solid, and the yield was (2.60g, 81%). This reaction was characterized using <sup>1</sup>H NMR (500 MHz, Chloroform-*d*): δ 2.75 (s, 3H), 7.57 (s, 1H), <sup>13</sup>C NMR (126 MHz, Chloroform-*d*): δ 19.27, 114.39, 150.29, 166.32.

#### A1.2 Preparation of 2,2'-diamino-4,4'-bithiazole<sup>36</sup>

To a two-necked round-bottom flask equipped with a stir bar and reflux condenser was added 1,4-dibromo-2,3-butanedione (4.00g, 16.40mmol), and thiourea (2.49g, 32.71mmol) in the same flask and filled with nitrogen gas under heating 65°C. To this, dry degassed methanol (50ml) was added. The mixture was allowed to reflux for approximately 3 hours. Once cooled, 50 ml of distilled water was added to the mixture, the solution was made basic using 5% Na<sub>2</sub>CO<sub>3</sub> until a pH of 9 was reached. The solution was suction filtered and the solid left to dry giving a light brown solid (2.03g, 83%). This

reaction was characterized using  $^1\text{H}$  NMR (500 MHz,  $\text{DMSO-}d_6$ ):  $\delta$  3.52 (s).  $^{13}\text{C}$  NMR (126 MHz,  $\text{DMSO-}d_6$ ):  $\delta$  102.86, 146.85, 168.55.

### **A1.3 Preparation of 4,4'-dimethyl-2,2'-bithiazole<sup>37</sup>**

To a 500ml three-necked round-bottom flask equipped with a stir bar and reflux condenser was added dithiooxamide (3g, 25mmol), and the flask was evacuated and purged. To this, dry degassed ethanol (120 ml) was added, forming a deep orange slurry. Chloroacetone (4.62g, 49.9mmol) was then added and the mixture was set to reflux. Once hot, the orange solid dissolved and the solution gradually became a deep burgundy color. The mixture was allowed to reflux for approximately 5 hours. The mixture was evaporated filtered and kept in the refrigerator to yield (4.03g, 82%).  $^1\text{H}$  NMR (500 MHz,  $\text{Chloroform-}d$ ):  $\delta$  2.17 (s, 3H), 7.03 (s, 1H)  $^{13}\text{C}$  NMR (126 MHz,  $\text{Chloroform-}d$ ):  $\delta$  18.40, 116.26, 153.75, 160.12.